Joint Centre for Mesoscale Meteorology, Reading, UK

The European Cloud-Resolving Modelling Programme (EUCREM) Summary report from the Coordinator

P. W. White

Internal Report No. 84

April 1998

Met Office Joint Centre for Mesoscale Meteorology Department of Meteorology
University of Reading PO Box 243 Reading RG6 6BB United Kingdom
Tel: +44 (0)118 931 8425 Fax: +44 (0)118 931 8791
www.metoffice.com

Designed and produced by the Met Office © Crown copyright 2001 01/0240 The Met Office logo is a registered trademark.

The European Cloud-Resolving Modelling Programme (EUCREM)

Summary report from the coordinator

By

P. W. White

(April 1998)

SUMMARY REPORT FROM THE COORDINATOR

By P. W. White

University of Reading, UK

SUMMARY

In Part B of the Final Report on the EUCREM project, section 1 describes the principal features of the EUCREM project. Section 2 provides a scientific overview of the topic, section 3 outlines the project work programme, and sections 4–7 describe the main achievements of the project with respect to the production of observational data-sets, cloud-resolving model simulations, single-column model simulations, and model intercomparisons. Finally section 8 summarizes the consequences and benefits of EUCREM, and provides suggestions for future research and collaborations.

1. THE EUCREM PROJECT

(*a*) *Objectives*

The European Cloud-REsolving Modelling project (EUCREM) was a 24-month project funded under the European Union's Fourth Framework Programme (Contract ENV4-CT95-0107) during the period 1 February 1996 to 31 January 1998.

The main aims of EUCREM were to exploit numerical cloud-resolving models, and observational data from field programmes, to improve the understanding of basic processes in convective clouds and, hence, to validate and improve methods of representing convection in global circulation models of the atmosphere.

The project was implemented with the purpose of contributing to the Work Programme in Environment and Climate (1994–1998) of the Science, Research and Development programme of the European Commission. It was designed to address the objectives and research tasks outlined in Paragraph 1.1.1—specifically sub-paragraph 1.1.1.4—(Basic processes in the climate system) of the Work Programme of Area 1.1 (Climate change and anthropogenic impact on natural resources) of Theme 1 (Research into the natural environment, environmental quality and global change).

EUCREM has had a direct input into the World Climate Research Programme (jointly sponsored by the World Meteorological Organization and the International Council of Scientific Unions) through its GEWEX* Cloud System Study (GCSS). Research collaboration between EUCREM and GCSS has been assisted by the EUCREM Coordinator's chairmanship of GCSS, and by EUCREM scientists being members of the GCSS Science Panel and actively participating in GCSS working groups and workshops.

EUCREM has involved 11 participating research groups and about 40 research staff; a central aspect of the project was to exchange observational data and results of model simulations between the project participants. With a project of this size, close and active project management was essential and, with this in mind, the Project Coordinator Prof K. A. Browning appointed a senior scientist Dr P. W. White to act as the part-time Technical Manager. To ensure close coordination of the research being carried out by the participating institutes, three workshops were held during the course of the project to discuss, and decide on, action plans relating to specific project milestones.

One of the important by-products of EUCREM has been the establishment of a network linking scientists within Europe involved in research on convection. The exchange of observational data, and of results from model simulations of convection, through this 'EUCREM Network' (using the facilities of the World-Wide-Web) has been instrumental in fostering this area of research within Europe. The blending of complementary aspects of expertise within the participating institutes has led to a deepening of the understanding of convective processes and to an enhanced ability to model them numerically. The participants have recognized the importance this coordinated activity and have agreed to continue this network after the termination of the EUCREM project; they will also endeavour to hold additional workshops on an annual basis.

* Global Energy and Water cycle EXperiment

(*b*) *The EUCREM project participants*

The EUCREM project was coordinated by the University of Reading and there were six Contractors:

- the University of Reading, United Kingdom. (UR);
- the Royal Netherlands Meteorological Institute, The Netherlands. (KNMI);
- the United Kingdom Meteorological Office, United Kingdom. (UKMO);
- the University of Manchester Institute of Science and Technology, United Kingdom. (UMIST);
- the Centre National de Recherches Météorologiques, France. (CNRM);
- the Deutsche Forschungsanstalt für Luft- und Raumfahrt, Germany. (DLR);

and five Associated Contractors:

- the European Centre for Medium-Range Weather Forecasts, United Kingdom. (ECMWF);
- the Institute for Marine and Atmospheric Research Utrecht, The Netherlands. (IMAU);
- the Max-Planck-Institut für Meteorologie, Germany. (MPIfM);
- the Laboratoire de Météorologie Dynamique, France. (LMD);
- the Instituto National de Meteorología, Spain. (INM).

In the remainder of this report participants will be referred to by their acronyms, as indicated above in brackets.

(*c*) *Milestones and deliverables*

The milestones and achievements of the EUCREM project are indicated in Table 1, and the deliverables are listed in Table 2.

TABLE 1. MILESTONES, TARGET DATES AND ACHIEVEMENTS FOR THE EUCREM PROJECT

Milestones	Target completion dates	Achievements
Complete the outline descriptions of observational case studies	May 1996	Observational case studies discussed at Workshop I
Conduct Workshop I to discuss the observational case studies and requirements for model diagnostics	May 1996	Workshop I was held at DLR on 13–14 May 1996
Complete and distribute the data-sets for the observational case studies (data-sets to be put onto the WWW)	August 1997	Data-sets were completed between the dates 5/9/96 and 13/10/96
Complete the cloud-resolving model simulations and conduct intercomparisons	May 1997	Simulations were completed in time for Workshop II
Conduct Workshop II to evaluate the cloud-resolving model intercomparisons	May 1997	Workshop II was held at KNMI on 1–2 May 1997
Develop and improve parametrization schemes using observational data and cloud-resolving model simulations	November 1997	Improved parametrizations were discussed at Workshop III
Complete parametrization tests and intercompare with cloud-resolving model simulations	November 1997	Tests and intercomparisons were completed in time for Workshop III
Conduct Workshop III to evaluate the intercomparisons	November 1997	Workshop III was held at ECMWF on 24–26 November 1997
Complete the simulations and intercomparisons, and present the full results in the Final Report	March 1998	Final Report submitted to the European commission
Identify papers for publication in the open scientific literature	March 1998	Papers for publication indicated in the Final Report

TABLE 2. LIST OF DELIVERABLES

Deliverables	Dates due
Data sets and documentation for observational case studies	August 1996
Progress Report	February 1997
Data sets and documentation for cloud-resolving model simulations	May 1997
Documentation of results of intercomparison of cloud-resolving model simulations and observations	May 1997
Documentation of results of intercomparisons of cloud-resolving model simulations and parametrizations	November 1997
Documentation of modifications to cloud-resolving models resulting from EUCREM	November 1997
Final Report	March 1998

The data sets and their documentation have been put onto the World-Wide-Web. Other documentation has been included in the Progress and the Final Reports submitted to the European Commission.

(*d*) *Project costs*

Table 3 presents a summary of the costs of the EUCREM project, together with details of the percentage funding grant from the CEC. Detailed figures are given in the Cost Statements prepared by each of the participating institutes.

TABLE 3. SUMMARY OF RESOURCES USED DURING THE PERIOD 1 FEBRUARY 1996 – 31 JANUARY 1998. ALL COSTS ARE IN KECU.

	First year costs 1/2/96–31/1/97	Second year costs 1/2/97–31/1/98	Full costs 1/2/96–31/1/98	CEC contribution %
CNRM	171	141	312	34
DLR	96	152	248	50
ECMWF	0	0	0	0
IMAU	32	31	63	100
INM	9	17	26	100
KNMI	0	44	44	100
LMD	30	33	64	50
MPIfM	9	70	79	100
UKMO	98	161	260	50
UMIST	44	45	89	100
UR	69	73	142	100
TOTAL	557	768	1325	

The maximum contribution by the CEC to the costs, as indicated in the EUCREM contract, was 806.400 KECU.

2. SCIENTIFIC OVERVIEW

(*a*) *The role of convection in the atmosphere*

In the context of atmospheric science the term 'convection' is normally (though not exclusively) reserved for thermally direct circulations that are driven by the action of gravity upon vertically-unstable distributions of mass (Emanuel 1994) (other thermally forced phenomena, such as those associated with horizontal temperature gradients within a *vertically-stable* environment, have rather different characteristic structures). However, even within this restricted definition convection takes many different forms and has a major influence on the atmosphere.

Convection is the principal mechanism enabling the transfer into the atmosphere of solar energy absorbed at the earth's surface, thereby setting up the large-scale meridional temperature gradients that drive the synoptic- and global-scale weather systems responsible for much of the atmospheric heat transfer between equatorial and polar regions. Within the tropics most of the cloud and rainfall is directly attributable to convection, but convection is also widespread at other latitudes. Convective

clouds are sometimes isolated, but they can also become organized into regular patterns or into more amorphous mesoscale complexes, or they can develop whilst embedded within larger-scale features such as fronts, squall lines and tropical storms. Deep convection, extending throughout the troposphere and sometimes well into the stratosphere, can be extremely vigorous and be accompanied by large vertical exchanges of heat, moisture and momentum; such cases are often associated with violent and hazardous weather. Cumulus clouds are an ubiquitous feature of the subtropical trade-wind belt where theyplay an important part in the ocean–atmosphere transfer processes. The lateral extents of the broad subtropical stratocumulus cloud sheets that form along the eastern boundaries of the world's major oceans are strongly influenced by interaction with cumulus convection. Small-scale convection within the boundary layer, as well as transferring heat, also mixes into the main body of the atmosphere pollutants, trace gases and particulates emitted at the ground surface from both natural and human-based sources.

Better understanding of convection and better ways of representing convective processes within numerical models of the atmosphere are high priority research objectives both for enabling climate models to provide more realistic depictions of phenomena that closely involve convection (such as global cloud and precipitation, intra-seasonal waves, monsoons, the El Nino/Southern Oscillation, the Hadley circulation, and the earth's radiative balance), and for improving the forecasting of severe local weather directly attributable to convection (such as floods, lightning, hail, tornadoes, tropical cyclones, strong winds, and aviation hazards such as turbulence, downdraughts and wind shear).

In summary, convection is recognized as being one of the key processes in the atmosphere because of:

- its ability to transport (relatively rapidly) heat, moisture, momentum and pollution between near-surface and higher tropospheric levels (and, in the case of deep convection, between the troposphere and stratosphere);
- its important role amongst the physical and dynamical mechanisms involved in the global circulation of the atmosphere;
- the impact of convective clouds on the radiative balance governing the earth's climate;
- the associated incidence of severe weather phenomena.

(*b*) *The parametrization of convection in large-scale models of the atmosphere*

Current weather-prediction and climate models have horizontal resolutions (of the order of 100 km) that are insufficient to resolve individual convective clouds (which have horizontal scales of 1–10 km). In contrast, the vertical structure of convection has scales that are comparable with the vertical scales of meteorological phenomena that the large-scale models are designed to resolve. Consequently, one of the difficulties in representing (or *parametrizing*) convection in large-scale models is that, unlike many other physical processes (such as turbulence or cloud microphysics), there is only partial scale separation within the context of the global model resolution, i.e. convection straddles the spectral boundary between scales that the large-scale model is capable of representing explicitly and those that are definitely subgrid-scale. The parametrization problem is further complicated by strong interaction with other subgrid-scale physical processes, and by the generation by convection of mesoscale circulations that interact in a non-trivial way with the large-scale flow.

A large variety of methods of parametrizing convection has been devised. All parametrization techniques used at the present time represent convection as a local process through adjustments to the atmosphere within vertical columns above the global-model grid squares; in consequence, such parametrizations are usually referred to as single-column models (SCMs). The parametrization schemes can be broadly categorized under three headings (Emanuel 1994).

- *Methods controlled by moisture budgets.* These techniques are based on the idea that convection must be accompanied by large-scale low-level influxes of water vapour to avoid exhausting the local supply of moisture within the boundary layer and leading to the removal of the potential instability necessary for sustaining the convective overturning (Charney and Eliassen 1964; Kuo 1965 and 1974; Anthes 1977; Krishnamurti *et al.* 1980; amongst others).

- *Convective adjustment.* Adjustment schemes are based on the principle that, in a statistical sense, convection tends to adjust the vertical thermal structure towards a neutrally stable equilibrium profile (Smagorinsky 1956; Manabe *et al.* 1965; Betts 1986; Betts and Miller 1986).
- *Mass-flux models.* Mass-flux models, attempt to model the ensemble of convective elements within the column above each grid square in a more detailed and elaborate way by taking account of, and predicting, a variety of quantities, such as upward and downward mass fluxes, mixing with the environment, cloud microphysics, precipitation, interaction with the boundary layer and with radiation, etc. The technique gets closer to an actual physical description of the life-cycle of convection than other methods (Arakawa and Schubert 1974; Fritsch and Chappell 1980; Raymond and Blyth 1986; Tiedtke 1988; Gregory and Rowntree 1989; and others).

There is, as yet, no consensus on the best way of representing convection in global atmospheric models, and within the EUCREM community examples of all three types of convective scheme have been tested. The key quantities of convective parametrizations that directly influence the large-scale dynamics are the apparent sources of heat, moisture and momentum due the convective processes (often referred to as $Q1$, $Q2$ and $Q3$) as computed from their flux divergences, though other aspects are also important for the radiation balance, such as the cloud fractional-area coverage and microphysical composition.

The testing and validation of convective parametrizations can essentially be undertaken in three ways (Randall *et al.* 1996):

- *Testing in extended runs of global models of the atmosphere.* This method of testing is extremely time consuming and expensive in computer resources, though it does provide the ultimate test of the usefulness of any proposed scheme.
- *Semi-prognostic test.* The parametrization is tested in a single column of a large-scale model by being supplied with initial profiles of the basic variables (either from output from model simulations or from observations) and by being integrated forwards for a single time step without feedback onto the prescribed input variables. The technique is computationally inexpensive, but it is not suitable for investigating mutual interactions with other physical processes.
- *Sub-model testing.* This is similar to the semi-prognostic test, except that the parametrization is integrated forwards for several hours, with full feedback on the enviromental profiles within the column; if appropriate, it may be forced with large-scale variables that change with time. The resulting evolution can be compared with observational data, or with simulations by very-high-resolution cloud-resolving models.

Whilst there is a role for all three of these methods of testing and evaluating convective parametrizations, it is the third method that has been emphasized within the EUCREM project proposal.

(*c*) *Validating SCMs using observational data bases and high-resolution cloud-resolving simulations*

The development and validation of SCMs has, in the past, been assisted by the availability of observations from field experiments. These data have been provided by specially instrumented research aircraft, space-based instrumentation, ground-based and airborne radars, and radiosondes dropped from aircraft or attached to balloons etc. Observational data sets for such studies have often been obtained during major international cooperative field experiments; the Barbados Oceanography and Meteorology Experiment (BOMEX) in 1969 and the GARP* Atlantic Tropical Experiment (GATE) in 1974 were early examples of such field programmes that provided data that have been (and still are being) widely used for developing better methods for representing convection in global models. More recent experiments, such as the Atlantic Stratocumulus Transition Experiment ASTEX in 1992 and the Coupled Ocean–Atmosphere Response Experiment of the Tropical Ocean/Global Atmosphere programme (TOGA-COARE) in 1993, as well as several other regional field experiments, are now being used more widely to broaden the range of types of convection being examined.

* Global Atmospheric Research Programme

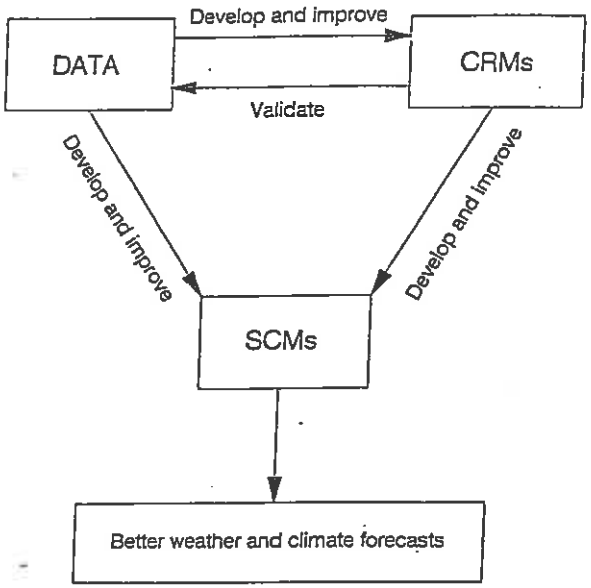

Figure 1. Schematic diagram illustrating the inter-relation between observational data and cloud-resolving model (CRM) simulations in providing validation data for improving single-column model (SCM) parametrizations in large-scale numerical weather prediction and climate models.

In recent years there has been increasing interest in the idea of using numerical simulations of convection to validate SCMs. One of the motivations for this development is that it is recognized that observations in the real atmosphere inevitably provide only somewhat limited snapshot samples of the full physical complexity of the processes involved, and of their consequences for the larger-scale structure. Recent advances in computer power have enabled the development of very-high-resolution mathematical models that, in principle, are able to represent realistically many of the physical processes controlling small-scale atmospheric phenomena such as convection. The earliest models of this sort were dry representations of boundary-layer turbulence, known as large-eddy-simulation models (LESs) (Lilly 1967; Deardorff 1971; Mason 1989; Nieuwstadt *et al.* 1991). More recently the concept has been extended to include the effects of cloud microphysics, turbulence and radiation, with the aim of simulating the life cycles of convective clouds. Convective processes can now be simulated with a useful degree of realism in cloud-resolving models (CRMs) or, when the model domain is large enough, cloud-ensemble models (CEMs). Provided that these models can be validated satisfactorily using actual observations of convection, they hold out the prospect of supplementing the field measurements so as to allow much more detailed analysis of the structure and mechanism of convection ant its larger-scale consequences than was available before. This combination of observational data and high-resolution model simulations (Fig. 1) promises to become a very powerful technique for improving our understanding of convection and for improving its representation in large-scale atmospheric models, and it was the exploitation of this approach that was the central theme of EUCREM project.

(*d*) *The synergy between EUCREM and the GEWEX Cloud System Study*

The objectives of the World Climate Research Programme's GEWEX Cloud System Study (GCSS) are to improve the understanding of the coupled physical processes within different types of cloud system, and to use this knowledge in the development of better parametrizations of cloud systems within climate and numerical weather prediction models (WMO 1997). Within the GCSS programme, CRMs, SCMs and mesoscale models are being exploited with the aim of studying the

interactive nature of cloud processes, rather than the individual systems themselves in isolation. The models, which are being developed and validated using observations from a variety of regional field experiments, are being used as test beds to develop improved understanding of the physical processes involved and to generate realizations of cloud systems in the form of 4-dimensional data-sets; these are being used, in turn, to develop and evaluate parametrization schemes for large-scale models.

The GCSS has established four working groups:

- *Working group 1.* Boundary-layer cloud systems dominated by turbulent boundary-layer processes;
- *Working group 2.* Cirrus cloud systems;
- *Working group 3.* Extra-tropical layer cloud systems;
- *Working group 4.* Precipitating convectively driven systems.

The research undertaken as part of the EUCREM project has provided input into the research programmes of GCSS working groups 1 and 4, and also simulations of two of the EUCREM case studies by GCSS research groups outside Europe have enhanced the EUCREM project's intercomparison exercise.

3. The EUCREM project work programme

(*a*) *Project work packages*

The EUCREM project work programme was split into two work packages (these map closely onto the programmes of the GCSS working groups 1 and 4):

- *Work package 1.* Non-precipitating convective cloud (stratocumulus and fair-weather cumulus);
- *Work package 2.* Precipitating convective cloud (cumulonimbus).

(*b*) *Observational data sets*

Five case-studies of convection were selected as the basis for the study, and initial data were prepared to enable simulations using CRMs and SCMs to be performed.

(i) *Work package 1.*

- *Case A: North Atlantic stratocumulus.* The case was an occasion of stratocumulus observed during ASTEX east of the Azores;
- *Case B: North Sea cumulus.* The observations were of cumulus clouds in an unstable airflow behind a cold front moving across the North Sea.

(ii) *Work package 2.*

- *Case C: Cold-air outbreak.* Convection in a cold airstream flowing off the ice sheet and over the Greenland Sea to the west of Spitzbergen was observed to change from a roll-cloud structure to a closed-cell structure as the boundary layer deepened downstream.;
- *Case D: Continental European thunderstorm.* Severe convective storms that caused tremendous damage in Germany and Switzerland were observed to form along a strong squall line to the north of the Alps;
- *Case E: Tropical western Pacific convection.* A 100-kilometre-long squall line occurred during the TOGA-COARE near Honiara island in the Pacific.

These observational cases are representative of very different types of convection, each with different key physical characteristics important for their simulation; details of each are summarized in section 4 of this part (Part B) of the Final Report — more extensive descriptions are given in Part C (I), (II), (IV), (IX) and (X).

(c) *Workshops*

The highly interactive nature of the EUCREM research project, which involved exchanging observational data and model simulations amongst the participants in accordance with a strict pre-defined timetable, dictated that several workshops had to be organized to discuss formats for data exchange, modifications to the plans and commitments by each of the research groups. Three workshops, involving representatives from all institutes participating in EUCREM, were held in order to discuss and coordinate the different phases of the EUCREM project.

(i) *Workshop 1.* The first workshop was held during the period 13–14 May at the Deutsche Forschungsanstalt für Luft- und Raumfahrt, Oberpfaffenhofen, Germany, and was attended by 24 participants. The objectives of the workshop were to consider the state-of-the-art of CRMs and SCMs, to discuss the proposed case studies, to decide on the definition of the initial conditions, the large-scale forcing and the diagnostics for the simulations, and to set out the commitments of each participating group.

Presentations were made by representatives of each of the participating institutes on their plans and objectives for the EUCREM project. Presentations were also made of the observational case studies: Case A by Peter Duynkerke (IMAU); Case B by Peter Jonas (UMIST); Case C by Phil Brown (UKMO); Case D by Thomas Hauf (DLV); Case E by Jean-Luc Redelsperger (CNRM). The main reservations expressed by the workshop participants were over the complexity of Case D; it was decided to concentrate the model simulations of Case D on the earliest stage of the squall line before it entered the Munich area. With this caveat, the workshop decided to proceed with studies of all five cases and agreed on the format for the initial data, boundary conditions and model characteristics for the simulations.

The commitments of each of the research groups for model simulations are indicated in Table 4. In the event, some of the participants exceeded their original commitments by conducting additional simulations, and results from additional simulations of Cases C and E were supplied by researchers in the USA and Japan who were not part of the EUCREM project; these have also been included in the intercomparisons, for completeness.

TABLE 4. INTENDED PARTICIPATION OF RESEARCH GROUPS IN MODELING STUDIES OF THE OBSERVATIONAL CASES A–E

Participant	Case A	Case B	Case C	Case D	Case E	Model
CNRM	-	-	yes	yes	yes	CRM
DLR	-	-	yes	yes	yes	SCM
	-	-	-	yes	yes	CRM
ECMWF	yes	yes	yes	yes	yes	SCM
IMAU/UU	yes	yes	-	-	-	CRM
INM	yes	yes	-	-	-	SCM
	yes	yes	-	-	-	CRM
KNMI	yes	yes	-	-	-	SCM
	yes	yes	-	-	-	CRM
LMD	-	-	yes	yes	yes	SCM
MPIfM	yes	yes	-	-	-	CRM
UKMO	-	-	yes	yes	yes	SCM
	-	-	yes	yes	yes	CRM
UMIST	yes	yes	-	-	-	CRM
UR	yes	yes	yes	yes	yes	SCM

In the above, SCM stands for single-column model and CRM stands for cloud-resolving model. IMAU and KNMI worked together on the CRM simulations of Cases A and B, with IMAU being the lead participant on Case A and KNMI being the lead on Case B.

It was also agreed that the responsibility for preparing and distributing computer data sets and documentation for observations and initial data for the simulations of each of the case studies would lie as follows:

Case A:	IMAU
Case B:	UMIST
Case C:	UKMO
Case D:	DLR
Case E:	CNRM

Each of these institutes undertook to receive, and place on the World Wide Web, the results of simulations of these cases, and to conduct intercomparison studies of the model output; a format for submitting model results, based on the one used for GCSS, was proposed by Peter Duynkerke (suggestions for additional model information were subsequently made by David Gregory (ECMWF) and Aad van Ulden (KNMI)). All participants planning to run CRMs agreed to produce their first results in time for the second EUCREM workshop in May 1997.

(ii) *Workshop 2.* The second workshop was held during the period 1–2 May at the Royal Netherlands Meteorological Institute, The Netherlands, and was attended by 31 participants. The objectives of the workshop were to discuss the CRM simulations of each of the five case studies and to decide if any modifications were needed before final versions of the simulations were intercompared with one another and with the observed data.

Presentations were made by each of the participants on simulation results that had been obtained so far. Each of the case-study coordinators reported on what needed to be done before the third EUCREM workshop, as follows:

- *Peter Duynkerke (Case A).* Studies needed to be made of the intercomparison of results from both coarse and fine resolution models.
- *Peter Jonas (Case B).* Two questions needed to be looked at: the influence of the initial profiles, and the averaging period that is appropriate for the results. Possible further runs to be undertaken were (a) repeat the simulations for a longer period of time, (b) re-run with a smoother water-vapour profile. After some discussion it was agreed that runs should be extended to 4 hours, and that the wind profile should be made more nearly geostrophic. It was also agreed that smoother humidity profile should be used. Hourly averages should be used for the last hour of the run (3–4 hours). There should be prescribed radiative cooling.
- *Phil Brown (Case C).* Points that arose were (a) the impact of low-level wind shear in producing rolls should be investigated (it was suggested that a wind profile 20 km behind the ice edge should be used for the initial conditions), (b) higher resolutions in the horizontal should be used to investigate the impact of the roll structure on convective transports, (c) the impact of cloud microphysics on the predicted cloud fraction should be studied, and (d) the consequences of a lack of geostrophic balance in the initial wind profile needed to be examined. It was proposed that new initial profiles should be provided for the CRMs and some new experiments along the above lines should be undertaken before the next workshop. Some higher-resolution runs were also desirable.
- *Thomas Hauf (Case D).* It was agreed that storms developing ahead of the squall line (as observed in Switzerland) should be examined, and that the modified Payerne sounding using a 500 m uplift for temperature (but keeping the same humidity profile) should be used. Sensitivity runs should be done with and without radiation, with and without the Coriolis effect, and with different specifications of the initial bubble perturbation. DLR would provide surface fluxes from the MM5 model simulation, together with large-scale forcing along similar lines to that of Case E. Runs should be done to 6 hours. Participants should also consider simulations on a moving nested grid in a 100×100 km domain.
- *Jean-Luc Redelsperger (Case E).* The intercomparison should include the GCSS studies of Case E as well as the EUCREM studies. Results had been obtained from 3 EUCREM participants (DLR, UKMO, CNRM), as well as from 6 GCSS groups outside the EUCREM project. CNRM were also doing a run with periodic boundary conditions to compare with the UKMO results. There was a need to compare the CRM results with cloud-scale observations and with Doppler radar data. A

methodology needed to be developed for comparing observational snapshots with hourly averages from the model simulations of the squall line. Results were needed from the SCMs to compare with the CRMs.

(iii) *Workshop 3.* The third workshop was held during the period 24–26 November 1997 at the European Centre for Medium-Range Weather Forecasts, UK, and was attended by 35 participants. The objectives of the workshop were to discuss the final results and intercomparisons of all SCM and CRM simulations, to decide on the content of the Final Report to the CEC and to consider proposals for any follow-on actions after the termination of the EUCREM project.

Presentations were made by all participants on their latest results, and the results of the intercomparison studies were discussed (full details are given in Part C of this report). The format and content of the Final Report were agreed. All participants welcomed proposals to continue cooperating after the end of the project, but there was no concensus to seek approval from the European Commission to continue EUCREM on a no-additional-cost basis; the possibilities for preparing a proposal for further funding would be reviewed, however, after the programme for Framework V had been published. Nevertheless, there was a welcome for the proposal that CEC funding should be sought for the holding of a fourth workshop in November 1998. The final day of the workshop was given over to an open scientific meeting where presentations were made of the EUCREM project as a whole.

4. Achievements of EUCREM: Observational data-sets

(*a*) *Case A: North Atlantic stratocumulus (data-set prepared and distributed by IMAU)*

The case study was of stratocumulus cloud over the North Atlantic which was in a transition stage, changing from a horizontally homogeneous cloud layer to a decoupled boundary layer with cumulus penetrating the stratocumulus deck from below. Observations were made by 7 research aircraft, from a research ship and from the islands of Santa Maria (Azores) and Porto Santo (Madeira). For this case study, the microphysical data that were of particular importance were those obtained by the NCAR *Electra* aircraft within the boundary layer during the first Lagrangian experiment of the Atlantic Stratocumulus Transition Experiment (ASTEX). Flights were made at different levels above, within and below the stratocumulus deck. The navigation was such that the aircraft remained roughly in the same airmass, and measurements were made at heights between 30 m and 2800 m above the sea surface. Microphysical measurements were made of droplet-size spectra, upward and downward longwave radiation fluxes, cloud liquid-water content, and temperature fluctuations. The data were considered suitable for preparing initial conditions for a 3-hour model simulation of the evolution of the boundary layer, starting at 0700 UTC on 13 June 1992.

Initial conditions for the model simulations were specified in the form of simplified vertical profiles (broadly consistent with the observations) of the two horizontal wind components, the liquid-water potential temperature, and the total water content. These were independent of height below cloud base, and varied linearly with height within and above the cloud, with jumps in the liquid-water potential temperature and the total water content across the inversion (the initial water content within the boundary layer was taken to be somewhat larger than observed in order to obtain the correct height of the cloud base). A uniform geostrophic wind was assumed, and a spatially uncorrelated random small perturbation was applied to the initial temperature at all grid points.

The friction velocity, and the heat and moisture fluxes at the surface, were given fixed values, and the net longwave radiation parametrization was a prescribed function of the liquid-water path (the net shortwave radiation was assumed to be zero). One problem was to agree on an appropriate value for the large-scale subsidence; it was decided at the first EUCREM workshop to adopt a value an order of magnitude larger than was suggested by the forecast model of the European Centre for Medium-Range Forecasts (ECMWF), because earlier experiments had indicated that such a value was necessary to ensure that the simulated boundary-layer depth remained close to the observed value.

All participants using CRMs were asked to use a standard configuration for their models, consisting of a 64×64 array of points with a horizontal grid length of 50 m. The vertical grid length was a uniform 25 m with 60 levels. The aim was to run simulations both with and without a parametrization of drizzle.

Details of the observations, the initial conditions for the simulations, and associated documentation have been placed on the World-Wide-Web at:

http://www.fys.ruu.nl/~wwwimau/EUCREM/eucrem.html

(*b*) *Case B: North Sea cumulus (data-set prepared and distributed by UMIST)*

Observational studies were made of fields of cumulus clouds over the sea in an unstable north-northwesterly flow behind a cold front moving southwards across the North Sea. The observations were gathered by the United Kingdom Meteorological Office *C-130* aircraft on 11 September 1991. Calculations, using bulk aerodynamic formulae, suggested that there were strong surface latent- and sensible-heat fluxes on this day, with the production of turbulence dominated by buoyancy (because there was almost no vertical wind-shear within the convective boundary-layer). The average separation of the cumulus clouds was 12 km, with a typical cloud depth of 1500 m and an average cloud-width at mid levels of 1.8 km. The cloud bases were at about 1000 m and some of the cloud tops penetrated above the inversion at 2200 m to heights of up to 2500 m . Cloud cover averaged 20% and light showers were observed, but the precipitation did not reach the ground. Aircraft data were obtained along straight and level runs above, within and below cloud base. The observations enabled estimates to be made of the vertical fluxes of heat, water vapour and liquid-water content, and of the turbulent kinetic energy, averaged over the in-cloud and cloud-free regions, and over the domain as a whole.

The initial data for the model simulations were specified so that all runs would be undertaken under nearly the same conditions. The initial temperature and humidity mixing-ratio profiles were smooth fits to the detailed observational profiles. However, problems in obtaining a sufficiently rapid spin-up in attempts to simulate the case led to a decision at the second EUCREM workshop to used a modified humidity profile that was moister than the observed state in at lower levels. Surface fluxes were prescribed and the roughness length was taken to be a value typical of light-wind conditions over the sea. An imposed large-scale divergence was applied to reduce the tendency in early simulations for the boundary-layer depth to increase in time throughout the integration period. The CRM modellers were requested to use a standard 100 m horizontal resolution.

Further details have been made available on the World-Wide-Web at:

http://meteo.phy.umist.ac.uk/~pdc/eucrem.html

(*c*) *Case C: Cold-air outbreak (data-set prepared and distributed by UKMO)*

A cold-air outbreak to the west of Spitzbergen commenced at around 1200 UTC on 9 March 1993, as a complex low pressure centre moved east over the North Cape and the Kola Peninsular, whilst high pressure was maintained over Greenland. At 0400 UTC on 10 March 1993 the northerly flow, which was almost perpendicular to the ice edge, extended to the coast of Norway, with a transition from roll clouds to closed cells at about 77.5°N, and to open cells at about 75.0°N. Between 0400 and 1200 UTC there was a distinct north–south convergence line at approximately 3.5°E associated with flow in the lee of Spitzbergen; this was characterized by deeper convection visible in satellite imagery. The air–sea temperature differences within the flow off the ice changed from −22°C to −12.5°C 420 km downwind. The main sea-surface temperature gradient was perpendicular to the wind direction, but remained between 1° and 3°C along the direction of the flow. The character of Case C differed substantially from those of Cases A and B in that it involved a boundary-layer depth growing steadily downstream in response to large surface heat fluxes, rather than one that was in an approximate steady state. Observations were made as part of the ARKTIS 1993 field campaign led by Dr Burghard Brümmer of the University of Hamburg Meteorological Institute. The observing

network included six-hourly radiosondes from ships located within the sea ice, and data from two instrumented aircraft.

Initial data for the model simulations were provided by composite soundings (derived using aircraft data below 2000 m and radio-soundings from ships above this level) for potential temperature, relative humidity and wind constructed at a location 50 km inside the ice edge, where the observed wind speed stayed almost constant over a 12 hour period and the surface temperature remained at about $-35°C$, with a shallow surface-based inversion.

The x-axis of the model simulations was set to be parallel to the mean wind direction within the boundary close to the ice edge. Following discussions at the second EUCREM workshop concerning difficulties with preliminary simulations, a number of alterations were made to the prescription of the initial data:

- the wind profile was simplified and set equal to the geostrophic wind; this retained the surface wind speeds, and the wind shear over the cloud layer, at values close to those observed and avoided excessive imbalance between the wind and pressure field;
- the roughness lengths for heat and moisture were reduced to 10% of that for momentum;
- the simulations used a fixed sea-surface temperature of $1.5°C$;
- the relative-humidity profile was altered so that it had a uniform specific humidity throughout the 400 m depth of the boundary layer.

A 60×60 array of grid points, with a horizontal resolution of 500 m, was proposed for the CRMs. An integration period of 20 hours was recommended; this corresponded to a fetch of around 500 km, comparable to the size of the domain over which aircraft observations were made.

Details about the initial data, and other documentation about the case study, have been made available on available on:

ftp://email.meto.gov.uk/pub/apr/eucrem/c/

(*d*) *Case D: Continental European thunderstorms (data-set prepared and distributed by DLR)*

On 21 July 1992 a strong squall-line evolved over eastern France and Switzerland ahead of a cold front. The storm system developed first as an unorganized pattern of isolated storms, some of which were supercells. Later the storms formed a line which propagated north-eastwards over Germany. The storms cause tremendous damage in Germany and Switzerland (where it caused the strongest hail event for decades), and there were 16 fatalities. The storm extended through the whole troposphere and 2 km into the stratosphere up to a height of 15 km.

The initial data for the model simulations were taken from the 12 UTC Payerne sounding, the closest sounding in space and time. Early attempts at simulating the storm showed considerable difficulty in triggering the convection. Other numerical studies, and also aircraft observations, suggested that the whole airmass had been lifted ahead of the cold front by about 500 m over a period of 2 hours, after the Payerne sounding had been made. After discussions at the second EUCREM workshop it was decided to modify the initial sounding by artificially lifting it 500 m, with the specific humidity of the lifted air being conserved.

It was recommended that the surface fluxes should be held constant throughout the CRM integration period; however, not all modellers did this. The storm was initiated using a warm bubble at the ground with a specified shape and strength. CRM modellers were encouraged to use as high a resolution as their computing facilities would permit: preferably with about 100×100 grid points, a horizontal resolution of 500 m and an integration period of 2 hours.

Because the convective system was embedded within an evolving synoptic-scale flow, it was considered essential that the SCMs were forced with large-scale tendency profiles that evolved with time; these were derived by Jean-Luc Redelsperger and Françoise Guichard from an integration with a CRM model with open boundary conditions.

Further details are available on:

http://www.pa.op.dlr.de/eucrem/

and on a CD-ROM distributed to all EUCREM participants

(e) *Case E. Squall line over the tropical western Pacific (data-set prepared and distributed by CNRM)*

A 100-kilometer-long squall line was observed to be oriented nearly perpendicular to the low-level shear vector and was travelling at a speed of about 12 m s^{-1}. It was well-sampled by airborne Doppler radar as it approached Honiara island during the mature and decaying stages of its life cycle. Two NOAA instrumented *P-3* aircraft and a *DC-8* aircraft sampled the squall line over a period of 5 hours. The near environment has been characterized by using both rawinsonde observations and *P-3* aircraft data. Satellite-derived cloud structures and surface-flux measurements are also included within the observational data set. The situation included convective and stratiform cloud, and it provided a good occasion for testing both the convective and large-scale cloud parametrizations. One aspect of particular interest was the impact on the large-scale flow of momentum transport by the convection.

The initial soundings for the model simulations were derived from a composite analysis of the available observations. The soundings were calculated on a stretched vertical grid extending up to heights of 21 km, with a resolution varying from 35 m at low levels to 750 m in the upper troposphere; all modellers were urged to use the same vertical grid if possible. A domain size of 100 km × 125 km was recommended, with a horizontal grid length of 1.25 km. In order to keep the convective system within the domain the model simulations were undertaken in a coordinate system moving with an appropriate fixed lateral speed.

Large-scale forcings were applied to the SCM simulations; these were deduced from runs of a CRM using open lateral boundary conditions.

Full documentation of the initial data has been made available on:

http://www.cnrm.meteo.fr:8000/gcss/

5. Achievements of EUCREM: Cloud-resolving model simulations

Eight of the eleven participants undertook to run CRM simulations. Four simulations were done for Case A (IMAU, INM, MPIfM, UMIST), four for Case B (INM, KNMI, MPIfM, UMIST), two for Case C (CNRM, UKMO), three for Case D (CNRM, DLR, UKMO), and three for Case E (CNRM, DLR, UKMO). In addition, one researcher from the USA produced a CRM simulation for Case C, and several research groups in the USA and Japan produced simulations of Case E. The following is a summary of their main results.

(a) *Cloud-resolving simulations by CNRM*

(i) *The cloud-resolving model.* CNRM has been using a non-hydrostatic cloud model that has been extensively tested on convective simulations. It has prognostic equations for momentum, subgrid turbulent kinetic energy, potential temperature, water vapour, cloud droplets, rain drops, ice, aggregates and graupel. The radiation scheme calculates longwave and shortwave heating and cooling in both clear and cloudy conditions, taking into account the effects of gases, aerosols and hydrometeors. The model can be run with open or periodic lateral boundary conditions. An appreciable amount of programming effort was devoted towards satisfying the EUCREM requirements for detailed diagnostic output from the simulations.

(ii) *Arctic cold-air outbreak (Case C).* The model was run over a 60 × 60 array of grid points with a horizontal resolution of 500 m. It used a simplified version of the microphysics code and was run to 20 hours. Strong surface heat fluxes generated at the initial time declined steadily to about half the initial values at the end of the simulation, whilst the latent-heat fluxes remained approximately constant throughout the period; aircraft observations indicated that this behaviour was broadly realistic. The along-flow and across-flow wind components evolved somewhat differently

(this was probably related to the orientation of the convective cells) but showed a decrease in shear and an increase in speed within the convective boundary layer. The boundary-layer depth increased steadily throughout the simulation, with convection penetrating the stable air above the cloud. Although the simulated temperature changes near the sea surface were fairly realistic, the rise in inversion height was greater than observed, possibly because the model simulation had no imposed large-scale subsidence. Heat, moisture and momentum budgets studies assisted in the interpretation of the simulation, and provided data for comparison with SCM simulations.

(iii) *Continental European thunderstorm (Case D).* Open boundary conditions were used to allow the development of the convective system. After many preliminary tests, an array of 100×100 grid points with a horizontal resolution of 1.5 km was adopted. The simulation used the full microphysics parametrizations and was continued for a period of 6 hours using a coordinate system that moved laterally with speeds comparable with those of the convective system itself. A single initial convective cell generated new cells, and intensified to occupy the entire region by the end of the simulation period. The storm developed into a line structure moving in the direction of the wind shear, with strong updraughts ahead and evaporative downdraughts to the rear. Changes in the direction of propagation could be related to down-gradient momentum transfer accelerating the low-level flow and modifying the shear orientation. The simulation was realistic in its prediction of the spatial scale of the storm, the propagation velocity, and the rainfall intensity. Budget calculations were made to provide large-scale forcings to the SCM simulations. Temperature and water vapour budgets suggested an equilibrium between the large-scale forcing and the convective response.

(iv) *Pacific squall line (Case E).* Many preliminary tests were performed, and eight different final simulations were made in order to study the sensitivity of the model to the ice-phase parametrization, the surface fluxes, the radiative processes, the domain size, and the lateral boundary conditions, and also to examine the differences between 2D and 3D simulations. The model runs indicated that it was possible to simulate the different stages of the squall line, which changed from a linear to a 'hooked' appearance during the period. Radar data indicated a double peaked structure to the vertical-velocity field; it was possible to simulate this realistically, but only if the ice-phase parametrization was included in the model. The momentum transports were quite different in the 2D and 3D runs, indicating that three dimensions were essential for simulating this apparently two dimensional squall-line structure.

(*b*) *Cloud-resolving simulations by DLR*

(i) *The cloud-resolving model.* The model used by DLR was version 5 of MM5, a model originating from Penn State University and the National Center for Atmospheric Research in the USA. It can be run both hydrostatically and non-hydrostatically, and there is a wide range of parametrization options to select for model runs. It can run in nested mode with the nest moving independently within a 'mother' model. The non-hydrostatic version was used for the EUCREM runs with open lateral boundary conditions. The microphysics scheme represents the effects of cloud water, rain, ice, snow and graupel, and the longwave and shortwave radiative scheme parametrizes heating and cooling in both clear and cloudy air.

(ii) *Continental European thunderstorm (Case D).* The simulation was performed with a mother model having 150×75 grid points and a grid length of 1.5 km, together with an embedded nested model with a similar number of grid points but with a resolution of 500 m. Two hours of simulation were obtained. The storm penetrated well into the lower stratosphere (15 km) at its mature stage, in agreement with observations, and the updraughts were predicted to be very strong (50 m s^{-1}) with significant falls of graupel at ground level (qualitatively consistent with reports of severe hail damage in Switzerland). The horizontal and vertical scales of the storm agreed with those deduced from radar observations. New cells formed both downstream and upstream with a longitudinal orientation along the wind direction; this was similar to the orientation of clouds seen on the satellite visual image. Simulated transport of inert tracers indicated that the storm produced a rapid vertical transfer from

the boundary layer into the storm's anvil and the lower stratosphere; this indicated the importance of such storms in facilitating troposphere-stratosphere exchange of pollution and trace gases.

(iii) *Tropical squall line (Case E).* A version of the model with 100 × 80 grid points and a 3.75 km resolution was used together with an embedded nested model having 100 × 136 grid points and a resolution of 1.25 km. The transformation of the squall line into an arc shape was well simulated, with back-building cell development and broadening of the squall line. The vertical-velocity fields showed a double structure, in agreement with the Doppler radar observations. There was some evidence, however, of excessive smoothing by the model diffusion process. The simulated tracer transport showed a slower vertical transfer than for Case D, with the tracer becoming distributed more evenly within the troposphere, rather than being transported into the anvil region of the storm.

(*c*) *Cloud resolving simulations by IMAU*

(i) *The cloud-resolving model.* The model used by IMAU was a so-called large-eddy simulation model. The model was incompressible and Boussinesq and had a 1.5-order turbulence closure scheme with a prognostic turbulent kinetic energy equation. The moist adiabatic processes were expressed in terms of the liquid-water potential temperature and the total water content. An 'all-or-nothing' scheme was used in the condensation parametrization. Radiative forcing was expressed as a function of the liquid-water path.

(ii) *North Atlantic stratocumulus (Case A).* The standard version of the model had a horizontal grid length of 50 m and a vertical resolution of 25 m; higher resolution runs were also made with horizontal and vertical resolutions of 25 m and 10 m, respectively. The higher resolution runs were similar to the standard run in the mixed layer, but a vertical resolution finer than 10 m seems necessary for resolving the entrainment process at the cloud top. Comparison of the resolved and subgrid buoyancy fluxes suggests that refinement of the horizontal resolution is also desirable. The model showed little sensitivity to changes in the nature of the initial random temperature perturbations, giving some confidence in the reliability of a single run. Tests of the sensitivity of the results to changes in domain size were made by running the model on domains four times, and sixteen times larger that the standard run. Whilst there were some differences between the standard and the larger-domain-size runs, it was concluded that the standard domain size was sufficiently large for reliable results to be obtained. There were larger differences between the runs with and without drizzle, with a lower entrainment rate being predicted in the former case.

A detailed investigation of energy spectra in the model simulations suggested that, in a version for which the domain scale was 16 times that of the boundary-layer depth, passive scalars do not automatically have the same scale as that of velocity perturbations, which is dominated by the scale of the boundary-layer height. The results also suggested that the dominant scale of passive-variable fluctuations is governed by the ratio of the entrainment flux and the surface flux of the scalar in question.

(*d*) *Cloud-resolving simulations by INM*

(i) *The cloud-resolving model.* INM has worked closely with CNRM in developing a non-hydrostatic mesoscale model, the Meso-NH model, which can also be run as a large-eddy simulation model. The model is anelastic and has an all-or-nothing condensation scheme, but no detailed microphysics scheme. It has a simplified second-order turbulence scheme with a mixing-length closure.

(ii) *North Atlantic stratocumulus (Case A).* The model was run using the standard configuration with a 64 × 64 array of grid points and a 50 m horizontal resolution, and a vertical resolution of 25 m, with 60 levels. The simulation maintained the stratocumulus deck with a steady rise in the cloud top throughout the simulation period of 3 hours. The potential-temperature and mixing-ratio profiles agreed reasonably well with the observations, but the cloud-water content was rather higher than was observed (possibly because of systematic underestimates in the observations). Profiles of turbulent kinetic energy, momentum flux, velocity variance, liquid-water potential temperature and

total-water flux have been examined. For the most part they agreed in general magnitude with the observations, but the considerable scatter in the measured values makes detailed comparisons inconclusive.

(iii) *North Sea cumulus (Case B).* The model was run over a period of 6 hours. During this time it did not reach a steady state until near the end of the run; maximum cloudiness was produced at about $2\frac{1}{2}$ hours followed by a minimum at $3\frac{1}{3}$ hours, and then a rise to a further maximum at $4\frac{1}{2}$ hours. The cloud-water content was, like the cloud cover, non-steady over the period of the simulation, and was consistently underestimated compared with the observations. The wind components, however, agreed well with the observations, as did the potential-temperature profile.

(e) *Cloud-resolving simulations by KNMI*

(i) *The cloud-resolving model.* The CRM model used by KNMI is the same as the one used by IMAU for simulating North Atlantic stratocumulus (Case A) (see subsection 5(c)(i) above). A full description has been given by Cuijpers and Duynkerke (1993).

(ii) *North Sea cumulus (Case B).* The model was run over a 6-hour period, but the first 2–3 hours should be regarded as the spin-up phase. When the clouds had formed sufficiently, after 3 hours of simulation, there was efficient transport of heat and moisture from the surface up to the inversion at a height of about 2 km. The net heating, after the spin-up period, was rather stronger than implied by the observations, probably because the longwave cooling was too low. The hourly-average fluxes fluctuated from hour to hour, and so most of the results were examined in terms of 3-hour averages. The cloud core (i.e. the positively buoyant part of the cloud) comprised about half of the cloudy area on average, and less than this at higher levels. The in-core vertical velocity was much larger than the vertical velocity in the negatively-buoyant parts of the cloud, especially near the inversion, and the mass fluxes decreased systematically with height. The cloudy parts were almost neutrally buoyant with respect to the environment, implying that there was very little build-up of CAPE (in contrast to the observed behaviour of deep convection).

(f) *Cloud-resolving simulations by MPIfM*

(i) *The cloud-resolving model.* The model used by MPIfM was an upgraded version of a large-eddy simulation model. It was Boussinesq and had prognostic equations for the three wind components (u, v, w), the liquid-water potential temperature, θ_l, and the total water content, q_t. The equations could be solved using a coordinate system moving with the geostrophic wind, and it had cyclic lateral boundary conditions and a Rayleigh-damping layer in the upper third of the domain. The model included representations of most of the physical processes occurring in the boundary layer. It had a simplified parametrization of radiative cooling and it could respond to imposed large-scale subsidence. The subgrid-scale turbulence parametrization had a transport equation for the turbulent kinetic energy. The cloud physics scheme distinguished between cloud and rain water content and parametrized the effects of autoconversion, accretion and self collection.

(ii) *North Atlantic stratocumulus (Case A)*

Statistical significance of the simulations. Ensemble runs (using initial data perturbed with different sets of spatially uncorrelated variations to the temperature field within the range ± 0.1 K) have been performed to give 21 realizations of the simulation. Examination of profiles of the predicted mean fluxes at a particular instant in time ($2\frac{1}{2}$ hours after the initial time) showed considerable spread amongst the ensemble members. The spread was reduced, but was still not negligible, when the results were displayed as 1-hour averages. Ensemble runs were also done for a domain 9 times larger in the along-wind direction. The spread was reduced still further for the 1-hour averages over the larger domain. These results indicate the need for care in interpreting results from a single model run, and demonstrate that averaging should be done over sufficiently large temporal and spatial domains.

Sensitivity to physical parametrizations. A number of runs were done on the standard sized domain (3.2 km × 3.2 km × 1.5 km) to test the sensitivity of the results to Deardorff's and Schumann's subgrid-scale schemes, and to Kessler's and Lüpkes's cloud microphysics schemes, as well as a 'no-rain' scheme. The Deardorff/no-rain run produced the deepest boundary layer and the largest liquid-water path. The impacts of the different subgrid schemes was small, but the primary effects of drizzle in the Kessler or Lüpkes runs was to reduce the buoyant production of turbulent kinetic energy, resulting in shallower boundary layers due to reduced entrainment rates. The removal of water by the drizzle lowered the maximum liquid-water content at the cloud top by 25%. The effects of latent heating within the cloud and evaporative cooling below was to produce an intermediate stable layer that decoupled the surface layer from the radiatively-driven turbulence at the cloud top.

Sensitivity to uncertainty in the initial data measurements. Simplified linear relationships between the variances of simulated quantities and the variances of measured environmental parameters were used to assess the sensitivity of the model to initial-data uncertainties. The coefficients in these relationships, which depended on the gradients of simulated quantities with respect to the observed parameters, were estimated from a limited number of ensemble runs. The exercise enabled error bars to be estimated for the simulations. Most of the simulated quantities appeared to agree with the observed data to within 90% confidence limits, but the drizzle predictions lay well outside these limits. It was concluded that the representation of precipitation processes within a numerical model of stratocumulus is difficult, and improving the results will prove to be a challenging task.

(v) *North Sea cumulus (Case B).*

Standard simulations. The model was run on a domain of 60 × 100 × 80 grid points using horizontal and vertical resolutions of 100 m and 50 m, respectively. Clouds appeared after 1 hour and the fractional cloud cover increased until 3 hours, after which it varied around a value of 30%. Rain formed during the simulation, but it evaporated before reaching the ground.

Sensitivity to initial conditions. Several sensitivity runs were made to investigate the impact of variations in the initial conditions; these involved increasing and decreasing the initial temperatures, increasing and decreasing the initial humidities, and increasing the imposed large-scale divergence. The fractional cloud cover was strongly sensitive to the initial conditions, with maximum values ranging from 5% to near 100% between members of the ensemble of runs. It was concluded that fractional cloud cover is not well suited for characterizing the nature of cumulus fields. Similar conclusions were made about the mean liquid-water content and the liquid-water fluxes, although momentum fluxes did not appear to be very sensitive to initial-data variations

(*g*) *Cloud-resolving simulations by UKMO*

(i) *The cloud-resolving model.* The model used by UKMO was a version of a large-eddy simulation model extended to enable it to be used for cloud simulations. The model was anelastic and had a positivity-preserving advection scheme. It used a modified version of the Smagorinsky–Lilly subgrid scheme that took account of the effect of moisture in determining the mixing length. The moist simulations predicted liquid-water temperature and total water content, as conserved variables. The Kessler scheme was used for autoconversion of cloud water into rain; rainfall, cloud ice, snow and graupel are prognostic variables.

(ii) *Arctic cold-air outbreak (Case C).* The model was run over a 20-hour period. Early runs of the model used an excessively high value of the roughness length; this resulted in large surface stresses and wind shears across the depth of the boundary layer. The simulations were, however, able to simulate the transition from horizontal-roll circulations to cellular convection at about 4–5 hours, as observed on the satellite pictures. However, the runs with a more physically reasonable value of z_0 failed to predict this feature, a problem that remains to be understood. A number of runs were done to test the impact of ice-phase physics, and it was concluded that the resulting significant differences in the microphysical structure of the cloud tops would probably have an impact on the radiative characteristics. Runs of the model with smaller horizontal and vertical grid lengths indicated little sensitivity of the results to model resolution, though the higher resolution runs had higher vertical velocities and more intense resolved motion during the first 2 hours of the simulation.

(iii) *Continental European thunderstorm (Case D).* The simulations were done using a 50 km × 100 km domain with a horizontal grid length of 1 km. The vertical resolution varied from 200 m near the surface to 390 m at high levels, the model top being at 25 km. Additional runs were undertaken to test the model's sensitivity to ice microphysics and to the surface fluxes. Simulated radar reflectivities compared well with radar observations. In runs with higher surface fluxes an evaporatively-driven downdraught was generated which interacted with the roll circulations in the boundary layer, and led to the triggering of secondary convective cells. A run with surface fluxes turned off had maximum updraughts of 10 m s^{-1} (compared with 25 m s^{-1} in the standard run), weak precipitation and no evaporatively-driven downdraughts. An examination of the vertical transport of a passive tracer released at low levels indicated rather lower concentrations in the anvil than expected, possibly because of excessive subgrid mixing in the updraughts.

(iv) *Pacific squall line (Case E).* A 3D run of the model for the required duration (7 hours) and the required domain (at least 400 km in the along-wind direction) was beyond the available computing resources, and so effort was devoted towards examining the model's sensitivity within a 2D-model format. Comparisons of runs with domain sizes of 400 km and 1000 km showed that the former did not sustain convective activity beyond 4 hours. The imposition of large-scale forcing alleviated this to some extent, but it led to spurious low-level cloud and precipitation. It was therefore decided that the larger domain was the most appropriate for subsequent tests on the impacts of radiation, ice-phase physics, and surface fluxes. Runs with ice-phase processes developed larger peak values of the updraughts at about 10 km during the first 4 hours. Two peaks occurred in the vertical-velocity field, but their separation was significantly greater than indicated by the Doppler radar observations. Rainfall rates at the leading edge of the squall line were not sensitive to the inclusion of ice-phase physics because most of the rainfall was generated by 'warm-rain' processes. The microphysical properties of the anvil were sensitive to the specification of ice-crystal bulk density.

(*h*) *Cloud-resolving simulations by UMIST*

(i) *The cloud-resolving model.* The model used by UMIST was the same model as was used by UKMO for CRM simulations of Cases C–E. Fluxes of water vapour and sensible heat were prescribed at the surface.

(ii) *North Atlantic stratocumulus (Case A).* 2D (3D) runs were carried out with the standard resolution of 50 m in the horizontal and 25 m in the vertical on a 64(×64)× 60 mesh of grid points. The model had no drizzle parametrization. The evolutions of the cloud-top height were similar in both 2D and 3D runs, and increased steadily during the run, with a near 100% cloud cover throughout. The 2D circulation patterns, as indicated by the vertical velocity fields, were rather different from those in the 3D runs because the former were constrained to be in one plane.

(iii) *North Sea cumulus (Case B).* Runs were carried out with a horizontal resolution of 100 m and a vertical resolution varying from 50 m near the surface to 150 m at the top of the model (4 km), on a horizontal domain of 60 km × 100 km. A Kessler drizzle scheme was included and a uniform 1°C day^{-1} longwave cooling was assumed. The evolutions of the 2D and 3D runs were quite different (unlike Case A). The clouds appeared in the 3D run after 45 minutes, but did not appear in the 2D run until $2\frac{1}{2}$ hours. Both runs indicated cloud tops rising from 1 km to $2\frac{1}{2}$ km by the end of the simulations, with the cloud cover increasing to a maximum of about 30%. Runs were also made with two passive tracers, one with a source below, and the other above, the inversion. The former was inhibited by the inversion and, when detrained from the boundary layer, became confined to a region few hundred metres above the inversion. When the second tracer was entrained downwards across the inversion it was rapidly mixed throughout the depth of the boundary layer to the surface. This inhibited its further detrainment back across the inversion, and so its concentration in the boundary layer steadily increased with time.

6. Achievements of EUCREM: Single-column model simulations

Seven of the eleven participants undertook to run SCM simulations. Five simulations were done for each of the Cases A–E: Case A (ECMWF, INM, KNMI, UKMO, UR), Case B (ECMWF, INM, KNMI, UKMO, UR), Case C (DLR, ECMWF, LMD, UKMO, UR), Case D (DLR, ECMWF, LMD, UKMO, UR), and Case E (DLR, ECMWF, LMD, UKMO, UR). The following is a summary of their main results.

(a) *Single-column simulations by DLR*

(i) *The single-column model.* The model used by DLR for the SCM simulations was a single-column version of the ECHAM-4 model. It had 19 levels and a time step of 40 min. Prognostic variables were temperature, water vapour and cloud water. The boundary-layer scheme had a TKE closure and surface fluxes were calculated using Monin–Obukov similarity theory. The stratiform cloud scheme was based on that of Sundqvist. The relative concentrations of liquid and ice within the cloud-water content were determined as a function of temperature. Cumulus convection was parametrized by a mass-flux scheme; CAPE closure was used for deep convection, and moisture convergence for shallow convection. Entrainment and detrainment rates depended on the type of convection.

(ii) *Pre-study investigation.* The climatology of deep convective events was studied in a 10-month perpetual-July run of a global circulation model. 400 deep convection events per month were found (about 14 per day). Deep convection is rare over most land areas, and shallow convection rather than deep convection dominates in the tropics and mid-latitudes. The concept of moisture convergence controlling deep convection over land seems questionable because such events appear to be characterized by deep instability and diurnal heating. Over oceanic areas nocturnal deep convection dominates, with rainfall maxima occurring during the night.

(iii) *Arctic cold-air outbreak (Case C).* The sea surface temperature was kept fixed and no large-scale forcing was applied. A deepening convective layer was predicted (in qualitative agreement with the observations) with the cloud base rising at about the same rate as the cloud top. The total cloud cover was about 10% lower than the observations but, after 2 hours into the simulation, an error in the numerical formulation caused negative humidities to appear and physical interpretation beyond this time was suspect.

(iv) *Central European thunderstorm (Case D).*

The basic simulation. The model was run for 6 hours with an interactive surface exchange scheme and external forcing in the form defined by CNRM. The radiation scheme was switched off. The surface forcing was strong enough to initiate convection at every time step. The maximum height of the convection was 11.3 km (about 2 km less than observed), but over the last 2 hours of the simulation the convective depth was only 6.3 km. The latent-heat flux divergence $Q2$ was balanced with the large-scale forcing in the mean but not locally, leading to drying at low levels and moistening above. In a sensitivity study with the surface exchange scheme altered to give lower surface fluxes, the convective type changed from deep to shallow convection in the middle of the simulation, the convective rain decreased, the cloud-liquid water increased and the large-scale rainfall increased.

Tracer transport studies. The two simulations (with large and small surface fluxes) were run with an inert tracer source near the ground. In the large-surface-flux run the tracer was quickly transported into the upper troposphere within a few time steps, but in the run with lower surface fluxes two maxima had appeared by the end of the run, one in the upper and the other in the lower troposphere. The former run had a broad area of organized entrainment, whereas the latter run had a narrow area indicating that clouds were all detraining at about the same level.

(v) *Pacific squall line (Case E).* The model was run for 7 hours with forcing provided from the CNRM CRM simulation. After 3 hours the model produced deep convection with cloud maxima at two levels, 10 km and 2.5 km. The convection warmed and dried the atmosphere, whilst evaporation of rain and cloud in the statiform-cloud scheme cooled and moistened it below 500 hPa.

A sensitivity study using runs with increased/decreased entrainment/detrainment showed that the cloud-top height, the rainfall rate and the surface latent-heat flux increased when the entrainment or detrainment were decreased. However, the model was more sensitive to changes in entrainment than to changes in detrainment.

(*b*) *Single-column simulations by ECMWF*

(i) *The single-column model.* The single-column model used by ECMWF was based on the ECMWF operational Integrated Forecasting System model. It had 31 levels and prognostic equations for the two horizontal wind components, temperature, specific humidity, cloud fraction and cloud liquid/ice water. In the soil there were prognostic equations for the temperature and water content of different soil layers, and for the skin temperature and water content. The model had detailed parametrizations for longwave and shortwave radiation, subgrid orographic drag, vertical diffusion and a Monin–Obukov surface layer. Convection was parametrized by a mass-flux scheme due to Tiedtke (1993).

(ii) *North Atlantic stratocumulus (Case A).* Two different types of simulation were performed, with and without drizzle. The mixed sub-cloud layer evolved in a similar way to that of a comparable CRM simulation, but the boundary layer did not deepen nor the cloud layer grow upwards, and the inversion was weak (probably because of the relatively coarse vertical resolution). The liquid-water profile was less realistic than in the CRM, though peak values were similar. When drizzle was included many features were somewhat similar. However, the liquid-water content was much reduced after 3 hours of the simulation. Comparisons with results of other SCMs suggested that the ECMWF model produced precipitation rates that are too large.

(iii) *North Sea cumulus.* The simulation was continued over a 6-hour period, and averages between 3 and 4 hours were examined and compared with CRM simulations and with the observations. After an initial spin-down, the model settled down with a cloud-top height of about 2 km, with occasional penetration of the convection into the inversion layer; the cloud top tended to deepen with time and was one model layer deeper by the end of the simulation. The main features of the $Q1$ profile were well captured, but the near-surface warming was underestimated. The $Q2$ profile indicated that the moistening in the cloud layer was too great at cloud base and too small at cloud top. Cloudiness predicted by the SCM was substantially too large, probably because of deficiencies in the algorithm that related cloud cover directly with the detrainment of cloudy air. The momentum flux divergences ($Q3$) agreed fairly well with those calculated from the CRM simulation. The cloud-base mass flux was too small and the heat and moisture budgets in the sub-cloud layer disagreed with those in the CRM. This may indicate the need to change the closure assumptions, and to reconsider the way that the convection and vertical diffusion schemes interact.

(iv) *Arctic cold-air outbreak (Case C).* The simulation was continued for a period of 20 hours with the effects of shortwave radiation switched off. Surface fluxes were calculated using the sea surface temperature and mixing length specified in the initial data. The model captured the sensible- and latent-heat fluxes well, and also the deepening of the convective layer, with modelled values agreeing with observations and CRM simulations. The precipitation in the SCM was larger than in the CRM simulations, resulting in a drier convective layer. Momentum transports were large, especially in the across-flow direction. There was little shear within the sub-cloud layer in the along-flow direction and the effects of surface drag dominated. Both components of the momentum flux were down-gradient, weakening the shear. Reasonable agreement was found with results derived from the CRMs, but the magnitude of the convective momentum fluxes was found to be sensitive to the specification of the in-cloud velocity at cloud base. As in (iii) above, some deficiencies suggested the need for further consideration to be made of the appropriateness of the closure scheme.

(v) *Central European thunderstorm (Case D).* The simulation was continued for a period of 6 hours using large-scale forcing derived by CNRM from their CRM run. Intense precipitation was predicted near the start of the simulation, declining rapidly over the first 40 minutes, with CAPE decreasing from 1000 to 200 J kg^{-1}. Convective precipitation dominated over most of the simulation, but stratiform precipitation increased and became larger near the end. Heat released by the parametrization

was in overall balance with the cooling induced by the large-scale forcing. The results suggested that the transport of condensed water from the convective scheme to the large-scale cloud scheme was too large, and that the results were somewhat sensitive to the treatment of evaporating rain.

(v) *Pacific squall line* The simulation was continued for a period of 7 hours, with imposed large-scale forcing derived from the CNRM CRM simulation. Following an initial burst of deep convection, only shallow convection occurred until 3 hours into the simulation, after which both the convective and stratiform precipitation increased, with the latter dominating. The convective heating ($Q1$) was in reasonable overall balance with the cooing due to the externally imposed large-scale forcing. However, near the melting level $Q1$ balanced only 30% of the cooling; this may be attributable to the parametrization not sufficiently offsetting the adiabatic cooling (due to the melting of ice) with the warming produced by the generated downdraughts. The peak magnitude of the convective mass flux agreed with the CRM simulation, but it occurred at a much higher level (5–6 km instead of 2 km). The SCM did, however, correctly produce the formation of an upper tropospheric cloud sheet.

(*c*) *Single column simulations by INM*

(i) *The single-column model.* The model used was a single-column version of the Meso-NH model (the model employed for INM's CRM simulations (see section 5(d), above)) except that the mixing-length scheme was changed to one based on the Bougeault–Lacarrère scheme.

(ii) *North Atlantic stratocumulus.* The original dry mixing-length calculation was change to one that took into account condensation and evaporation; this change improved the simulation of this case study. A steady state was reached during the third hour of the run, with the cloud-top level stabilizing at 720 m. The liquid-water path was larger than in the CRM, but the cloud-water profile was well modelled, with the maximum at the correct height. The turbulent kinetic energy budget indicated that the main production was due to shear near the ground, to buoyancy inside the cloud, and to turbulent transport at the cloud top. The large production of turbulent kinetic energy near the surface was not in agreement with the CRM, but the turbulent flux profiles were close to CRM values. A sensitivity run using the Sommeria–Deardorff subgrid-scale condensation scheme made very little difference to the results.

(iii) *North Sea cumulus (Case B).* A steady state was reached by 2.4 hours, but the cloud cover oscillated between 5% and 22% with a similar magnitude (but not phase) to that of the CRM simulation. Most of the mean profiles agreed quite well with the CRM results. The water-vapour profile was not as dry in the SCM simulation because the cloud generation was not so active. The wind components were well simulated and compared well with those in the CRM simulation.

(*d*) *Single-column simulations by KNMI*

(i) *The single-column model.* The model used was a 1D version of the RACMO (Regional Atmospheric Climate Model) developed at KNMI. The physics package was based on the ECHAM4 physics. This used a modified version of Sundqvist's cloud scheme, with prognostic equations for water vapour and liquid water. The cloud fraction was computed diagnostically as a function of the relative humidity. The convective parametrization used was the Tiedtke mass-flux scheme. Shortwave radiation was switched off. The subgrid turbulence scheme employed a prognostic equation for the turbulent kinetic energy.

(ii) *North Atlantic stratocumulus (Case A).* The model was run with a vertical grid length of 25 m and a time step of 1 s. The cloud-top height rose from 700 m to 800 m in three hours, with a mean entrainment rate of 2.1 m s^{-1} during the last hour. The buoyancy flux was a little low when compared with the CRM run, indicating that the entrainment was a bit high. The turbulent kinetic energy profile was too smooth and had a maximum near cloud base, in contrast to the CRM simulation which had a significant peak near the cloud top.

Time-step sensitivity. The results were very sensitive to the time step used; with a time step of 30 s the entrainment was much too high, and the cloud top reached 800 m after only $2\frac{1}{2}$ hours

and there was a rapid decrease in the cloud thickness after the third hour. It was demonstrated theoretically that a combined implicit and explicit time integration scheme may not converge to an exact solution if a long time step is used. A modified scheme was developed that removed this sensitivity to the time step. The new scheme gave improved results for Case A using a time step of 30 s.

(iii) *North Sea cumulus (Case B).* The SCM had difficulty in maintaining the conditionally-unstable air; the vertical structure of the sub-cloud and conditionally-unstable air became well mixed with a strong inversion at 2 km. The reason for this could be attributed to unrealistic interaction between the planetary boundary-layer scheme and the mass-flux scheme, which had a moisture-convergence closure. The model also produced cloud cover and liquid-water contents that were an order of magnitude larger than the CRM results, partly because of the same reason and partly because of deficiencies in the cloud scheme itself.

(*e*) *Single-column simulations by LMD*

(i) *The single-column model.* One of the main aims of the LMD model simulations was to develop and test the Emanuel mass-flux convection scheme. This differs from the Tiedtke and Bougeault schemes in having multiple updraughts fed by entrainment as well as the main updraught and an evaporatively driven downdraught, and in allowing detrainment to occur at all levels. The model also had a dry convective adjustment scheme, a large-scale condensation scheme (but no large-scale cloud scheme), and a conventional K-diffusion scheme in the vertical. Water-vapour and liquid-water content were prognostic variables, but there was no ice-phase physics.

(ii) *Central European thunderstorm (Case D).* The simulation was performed with a fixed surface temperature, but no temperature perturbation was necessary to initiate the convection. The convection developed smoothly with the vertical profile of the convective mass flux having similar magnitudes to that of the CRM simulation. $Q1$ and $Q2$ profiles also agreed fairly well, but the average vertical velocity was not consistent with the large-scale forcing. The cloud-water mixing ratio had two peaks at 600 hPa and 350 hPa (though, in the CRM, the upper one corresponded to ice clouds). The rainfall was mainly convective rather than stratiform.

(iii) *Tropical squall line (Case E).* A temperature perturbation to trigger the convection appeared to be essential for this case. The convection developed smoothly. After 6 hours the $Q1$ profile had a peak at 400 hPa whilst the $Q2$ profile had two peaks at 400 hPa and 800 hPa, the upper one being due to condensation of detrained water vapour. The vertical convective mass flux corresponded to an average vertical velocity slightly larger than that implied by the large-scale forcing, with a maximum at 400 hPa in agreement with the CRM results. Precipitation was mainly due to convection rather than stratiform processes, and the cloud-water mixing ratio was in good agreement with the CRM simulation.

(*f*) *Single-column simulations by UKMO*

(i) *The cloud-resolving model.* The single-column model was a 1D version of the UK Meteorological Office's Unified Model that is used operationally for climate simulations and numerical weather prediction. The model contains parametrizations of subgrid-scale cloudiness, radiation, boundary-layer turbulence (with a first-order closure), large-scale precipitation and a mass-flux convection scheme.

(ii) *North Atlantic stratocumulus (Case A).* The global version of the model tends to underpredict stratocumulus, and so the case study was used to investigate the model's sensitivity to vertical resolution and to changes in the boundary-layer scheme when simulating stratocumulus cloud.

Sensitivity to vertical resolution. The standard 19-level version of the model has insufficient vertical resolution to represent the cloud or boundary-layer structure adequately. A second run with 30 levels sharpened the inversion and improved the realism of the cloud simulation, which had a maximum cloud liquid-water content in the topmost of the 3 levels within the cloud. In both runs

the cloud gradually evaporated and the inversion lowered, with the timing of the cloud dispersal being similar. A run of the 30-level version with precipitation suppressed indicated that, without drizzle, the cloud persisted for about 2 hours longer. Also, convection occurred more readily and the boundary-layer mixing was reduced.

Sensitivity to the boundary-layer formulation. A run was made with a revised boundary-layer formulation in which the mixing coefficients were specified as functions of the surface-layer scaling velocities and of the height of the inversion, and a parametrization of cloud-top entrainment was included. The evolution of the cloud layer was similar in both the standard and the revised formulation, but the new scheme removed the intermittent convection and maintained the cloud layer by boundary-layer mixing. A run of the 30-layer version using the new boundary-layer scheme, but with precipitation suppressed, again showed a very similar evolution to that of the standard version.

(iii) *North Sea cumulus (Case B).* In the 19-level version of the model, the convection did not start to operate until 4 hours into the simulation. After the convection started there was a strong burst at about $4\frac{1}{2}$ hours followed by a more steady phase. The convection was generated from about the same level as the observed cloud base, but the mass fluxes were much smaller than those in the CRM simulations. There were large vertical transports of moisture by the boundary-layer scheme, possibly because of the use of a local, rather than a non-local, scheme for determining the eddy viscosities.

(iv) *Arctic cold-air outbreak (Case C).* The SCM had 14 levels and a model top at 5 km. The initial large surface evaporation and shallow boundary layer led to snow being diagnosed very quickly by the large-scale cloud scheme. The surface fluxes were larger than in other simulations of this case, and so a second run of the model was performed with a revised surface exchange scheme in which the transfer coefficients were based on surface-layer similarity. In both runs the loss of water from the column by precipitation was a significant fraction of the total evaporation from the sea surface. Similar proportions were produced from the large-scale cloud and the convection schemes, but the revised version of the model produced rather more as large-scale precipitation. The surface fluxes were significantly smaller for the revised version. Both runs produced intermittent large-scale precipitation after 10 hours.

(v) *Central European thunderstorm (Case D).* A 31-level version of the model was used for this case study. Two runs were performed, the first using the standard closure for the convective parametrization and the second using a CAPE closure. The standard scheme produced a burst of heavy precipitation after about $2\frac{1}{2}$ hours, and precipitation from the large-scale cloud started at about 4 hours and increased with time thereon. The run with CAPE closure was much smoother, but convection started earlier after about 1 hour into the simulation and increased steadily until the end of the run. Large-scale rainfall began at about the same time in both runs. The profiles of $Q1$ were similar in shape, with peaks at 7 km, but the magnitudes were larger in the CAPE-closure run. The external forcing was not balanced by the convective scheme alone; the contribution by the stratiform-cloud scheme was important, above 3 km for the standard run and above 5 km for the CAPE run.

(vi) *Pacific squall line (Case E).* A 31-level version of the SCM was used for the simulation of this case, with the model top set at 40 km. As with Case D, two versions of the model were run, one with the standard convection-scheme closure and the other with CAPE closure. The standard run produced a burst of convection at the start of the simulation, and the precipitation rate increased after 3 hours, all the precipitation being produced by the convection scheme. The evolution of the CAPE-closure run was similar, but much smoother and without the initial burst of convective activity. Also, unlike the standard run, the CAPE run produced large-scale precipitation after about 3 hours; this increased with time and eventually exceeded the convective precipitation. The total precipitation in both runs agreed with the CRM simulations. In the standard run the contribution to $Q1$ came mainly from the convective scheme, but in the CAPE run both the convective and the stratiform schemes contributed more or less equally.

(*g*) *Single-column simulations by UR*

(i) *The single-column model.* A single-column version of the UGAMP global climate model was used for the EUCREM simulations in order to develop and evaluate the Betts–Miller convection scheme. The model also contained parametrizations for a local stability-dependent turbulence scheme, a precipitation scheme that removes supersaturation, a diagnosed cloud scheme and a radiation scheme. The SCM was modified to allow external forcing and prescribed surface fluxes. Cloud fraction and cloud ice/water content were diagnosed variables.

(ii) *North Atlantic stratocumulus (Case A).* The initial data were modified to replace cloud water by humidity at saturation, and to use diagnosed cloud water in the specified longwave cooling algorithm (the resultant longwave cooling was less than prescribed but was spread over the two in-cloud levels rather than just at the top). The evolution of $Q1$ and $Q2$ showed that convection was maintained for 13 hours, ceasing shortly after the longwave cooling had declined because the rather weak moistening of the cloud layer was unable to overcome the drying by the imposed large-scale subsidence. The shallow convection scheme penetrated through the cloud layer and into the inversion, but an analysis of the mixing of conserved variables has revealed some shortcomings of the scheme.

(iii) *North Sea cumulus (Case B).* The parametrized turbulence in the SCM began only in the surface layer, but convection was initiated immediately. The resulting convective mixing then occurred within the cloud layer and across the inversion, but small-scale turbulence from the surface layer took 1–2 hours to fill the sub-cloud layer. The CRMs, however, took 2 hours or so to develop mixing from the surface through to the inversion, leading to rather different thermodynamic profiles; this made comparison between the SCMs and CRMs difficult. The evolution of the simulation was examined over a period of 12 hours. There was intermittency in the cloud-base level, probably because of the relatively coarse model resolution. The $Q2$ profiles remained noisy because of poor overlap between the parametrized turbulence and the convection. The initial sensitivity suggested the need for a technique to represent mixing across the inversion more realistically, such as cloud-top entrainment instability. The cloud cover was diagnosed to be between 10% and 40%, and was sensitive to the number of levels in the cloud.

(iv) *Arctic cold-air outbreak (Case C).* The model used the Charnock relation at the sea surface, rather than the prescribed roughness length, since this gave almost the same fluxes. The deepening of the cloudy boundary layer in response to the strong surface warming was successfully simulated. Shallow convection was initiated at the start, but convective precipitation was formed when the cloud top reached 800 hPa after about 11 hours. After this, the convection alternated between the two types, but with a fixed cloud top. The boundary layer became saturated soon after the initial time, and remained so thereafter. The evolution had an intense 4-time-step variation in the parametrized heating and moistening because of time lags in the interaction between the turbulence and the stratiform condensation schemes.

(v) *Central European thunderstorm (Case D).* This case was successfully simulated for a period of 6 hours. The model excluded radiation. Simulations were performed using constant surface fluxes (both 100% and 80% of the prescribed values), and also with interactive surface fluxes. The evolution of precipitation at the surface was smooth with little sensitivity to surface forcing. With interactive surface fluxes, the land surface cooled rapidly due to the strong initial turbulent heat loss and the lack of radiative forcing. Despite this cooling, the convection and the precipitation remained almost as intense as when the surface fluxes were prescribed. There was no noticeable spin-up, and deep convection was involved from the start. The convective forcing soon saturated the upper troposphere, and stratiform precipitation formed and evaporated below, extending the saturated layer downwards to reach the ground during the last hour of the run. The turbulence and convection interacted in such a way as to produce little intermittency, but during the last hour the convective-downdraught parametrization strongly stabilized the sub-cloud layer, and some intermittency occurred in the prescribed-surface-flux runs. The diagnosed cloud fraction and water content did not seem to link up well with the convective and stratiform processes.

(vi) *Tropical squall line (Case E).* Two versions of the model were run, one with a convective-adjustment time of 1 hour and the other with 2 hours. The simulations were continued over a period of 7 hours. The evolution was smooth but there was a marked spin-up in the first hour, particularly for the 1-hour-adjustment run. When surface fluxes were omitted from the model the deep convection ceased after 3 hours and became intermittent, despite the large-scale forcing. When radiation was omitted instead, the deep convection remained continuous, with very little difference to the control integration. The largest effect of the radiation was near the cloud top, however the convective-heating profile was noisy and the cloud top fluctuated; this became worse when radiation was included. As in Case D, the diagnosed cloud fraction and water content appeared to have unrealistic vertical profiles. Complete cloud cover was diagnosed near the cloud top, indicating the presence of an anvil.

7. Achievements of EUCREM; Model intercomparisons

A central aspect of EUCREM project plan was to compare the simulations by the CRMs and SCMs with one another and with the observations. Each of the participants was requested to send in their results electronically using a pre-defined format to the institutes that provided the original observational data for Cases A–E. It was then the task of these institutes to compare the results and to produce reports on their conclusions. The following is a summary of their findings.

(*a*) *Intercomparison of simulations of Case A by IMAU*

The results from four CRMs (IMAU, INM, MPIfM, UMIST) and five SCMs (ECMWF, INM, KNMI, UKMO, UR) were available for intercomparison. In addition IMAU provided results from a high-resolution CRM run.

Cloud-resolving models. A number of predicted quantities characterizing the observational case study were extracted as averages over the third hour of the simulation, and were compared with one another. The profiles of liquid-water potential temperature and total water content all agreed closely with one another, with inversion heights ranging from 776 m to 805 m, some 100 m above the initial value (662 m). All the models predicted an adiabatic liquid-water profile; the observations suggested liquid-water contents that were less than the adiabatic value, possibly because of systematic underestimates by the aircraft instrumentation or because of the presence of drizzle.

There was close agreement amongst the models in their predictions of longwave fluxes but, due to limitations in the vertical resolution, the jump in the longwave flux at cloud top was spread over two levels; this made the buoyancy flux not very well resolved near the cloud top. Three of the models gave very similar buoyancy-flux profiles that were in reasonable agreement with observations, but one model gave larger buoyancy fluxes throughout the depth of the boundary layer. All models indicated local dissipation-rate maxima at the sea surface and at the inversion, but all gave larger values than were implied by the observations. Three of the models gave vertical-velocity-variance profiles that agreed reasonably well with the data, but one model had values that were too large.

Values of the entrainment velocity deduced from the simulations varied from 1.79 cm s^{-1} to 2.02 cm s^{-1}, rather larger than the value of 1.2 ± 1.0 cm s^{-1} deduced from the observations. Both the observations and the simulations gave values of about 0.5 for the updraught-area fraction, and the simulated mass fluxes were fairly realistic. The vertical-velocity spectra in the middle of the cloud layer indicated that the most energetic eddies had horizontal scales comparable with the boundary-layer depth, whilst the corresponding water-flux spectra indicated that most of the flux was transported by eddies with sizes comparable to the horizontal dimension of the domain.

The modelled drizzle rates were an order of magnitude smaller than observed, probably because of spatial and temporal intermittency (this suggestion is supported by the fact that the aircraft flight just before the one used for generating the initial data measured drizzle rates that were comparable with those in the simulations). Comparisons between runs with and without drizzle indicated that the buoyancy fluxes and entrainment velocities were not very sensitive to the process.

Single-column models. Two of the SCMs were run at the standard 25 m vertical resolution, whilst the other two were run at the coarser vertical resolutions used operationally. All the models predicted a solid stratocumulus layer, and three produced liquid-water content profiles agreeing

with the CRM simulations and with the observations. However, the buoyancy fluxes produced by the SCMs showed very little resemblance to the CRM simulations. Some of the models indicated and increase in time of the total water content within the boundary layer, whilst others produced a decrease (however, the CRMs all indicated a decrease).

In summary, all the models were moderately successful at simulating the broad characteristics of the stratocumulus-topped boundary layer, though scatter in the observational data due to spatial and temporal intermittency made detailed verification difficult. Overall, the CRMs produced fairly self-consistent and realistic simulations, except for the predictions of drizzle. The SCMs failed to produce buoyancy fluxes that agreed with the SCMs.

(*b*) *Intercomparison of simulations of Case B by UMIST*

Results from five CRMs (INM, KNMI, MPIfM, UKMO, UMIST) and five SCMs (ECMWF, INM, KNMI, UKMO, UR) were available for the intercomparisons.

All the CRMs took about 2 hours to reach a steady state, after which there were fluctuations associated with the growth and decay of individual convective clouds. Examination of averages over 3–4 hours indicated that the profiles of turbulent kinetic energy (TKE) and cloudiness were broadly similar. The SCMs, however, grossly overestimated the cloud cover compared with the observations; they tended to predict 100% cloud cover with small cloud-water contents. There was close agreement between the SCM results and the CRM predictions of the potential temperature and humidity profiles, apart from one model which failed to predict the onset of convection until a later time. Within and below the cloud layer the models agreed to within about 0.3 K, though there were some systematic differences that could be attributed to different lower boundary conditions. Both the simulations and the observations indicated that the boundary layer was not in a steady state.

Three of the CRMs agreed well with one another in their simulations of profiles of liquid-water content and cloud fraction, but the other two differed considerably. Compared with observations, the CRMs produced the correct shapes of the profiles, but they underpredicted the magnitudes by a factor of 5; clearly liquid-water and cloud fraction are sensitive parameters for comparing models. The SCMs predicted much higher values than the CRMs, but with considerable differences between them. The CRMs failed to predict the maximum cloud cover in the middle of the cloud layer; other experiments have suggested that cloud-cover and liquid-water profiles are sensitive to the detailed structure of the initial humidity profiles.

The CRMs' simulated TKE profiles were in qualitative agreement with observations, but they failed to produce the strengths of the maxima at cloud top and below cloud base; the latter needs further observational study to understand its origin.

The SCM and CRM simulations had similar heat- and water-flux profiles. The observed values were similar in magnitude, but the small values just above cloud base were not produced in the simulations. The models showed great consistency in their predictions of momentum fluxes, though there were no observations for comparison.

The key parameters for representing transport processes correctly in large-scale models are the flux divergences of heat, water and momentum ($Q1$, $Q2$, and $Q3$). There was good agreement between the CRMs in general in their predictions of $Q1$, but there were differences in the locations of the maxima and minima. However, the SCMs differed considerably and they all failed to produce the maximum around cloud top. The SCMs also disagreed with the CRMs in their predictions of $Q2$. There was, however, much greater consistency in the prediction of momentum-flux divergences.

In summary, the CRMs produced good representations of the development of the boundary layer as a whole, but there were evidently severe problems in simulating cloud cover and cloud-water content. The SCMs also had some deficiencies in their representations of flux divergences of heat and moisture.

(*c*) *Intercomparison of simulations of Case C by UKMO*

Results from two CRMs (CNRM, UKMO), plus an additional CRM simulation performed by the National Center for Atmospheric Research USA, and three SCMs (ECMWF, UKMO, UR) were

available for intercomparison.

The early simulations of Case C showed that the CRMs could predict the observed transition from horizontal roll circulations to cellular convection, but only if unrealistically high values of the roughness length were used. With more correct values of the roughness length, this feature was not present in the simulations.

There were significant differences in the magnitudes of the surface fluxes predicted by the CRMs and SCMs, but all predicted a large initial heat flux that steadily declined by about 59% after 20 hours, and an approximately constant latent-heat flux throughout the period. All models gave good simulations of the boundary-layer evolution over the first 12 hours, but they produced larger deepening than observed by 20 hours; this may have been because of the absence of imposed large-scale subsidence in the model simulations. There was a significant spread in the range of latent- and sensible-heat fluxes predicted by the models. However, differences in the water-vapour tendencies in the simulations could be largely attributed to differences in the surface heat forcing.

The predicted surface precipitation rates were similar to one another, but the evaporation of precipitation differed substantially from model to model. Most of the observed precipitation was in the form of snow, but different assumptions about the size distributions and fall speeds of precipitates led to differing evaporation rates and, in turn, to differing cooling rates. However, larger evaporative cooling rates led to more vigorous convection and greater heating by resolved-scale motion, which largely offset the excess cooling.

The models differed in their predictions of the extent of the penetration of the inversion by the convection. This process is largely governed by longwave radiative cooling at cloud top, and models that produced the highest cloud water contents tended to have larger longwave cooling and deeper penetration through the inversion. However, another factor was the strength of the convective updraughts; a simulation with higher vertical resolution produced stronger updraughts and greater inversion penetration.

(*d*) *Intercomparison of simulations of Case D by DLR*

Results from three CRMs (CNRM, DLR, UKMO) and five SCMs (DLR, ECMWF, LMD, UKMO, UR) were available for intercomparison. The three CRMs differed substantially in their configurations, and this has had an impact on the ability to make meaningful comparisons of the results of the simulations. In particular, domain-averaged quantities had to be multiplied by scaling factors before they could be compared.

All the CRMs predicted the development of a severe storm with large vertical velocities having maxima ranging between 30 m s^{-1} and 50 m s^{-1}, and realistic cloud-top heights of around 13 km with overshoots up to 1.5 km above. A comparison between a run with the specified surface fluxes and one with larger surface fluxes demonstrated the relationship between increased vigour of the storm and larger surface fluxes. The observed storm propagation speed of 10 m s^{-1} was a little greater than the simulated speeds which ranged between 6 m s^{-1} and 9 m s^{-1}. One of the CRMs produced output of simulated radar reflectivity; this agreed well with the observed maximum value of 65 dBZ.

There were differences between the CRMs in their predictions of the storm structure. The storm cells were observed to have longitudinal structures aligned along the direction of the mean wind. The simulations disagreed with one another; one produced a longitudinal cell structure, one produced a lateral structure to start with and a longitudinal structure later in the simulation, whilst the third CRM produced a lateral structure throughout the simulation.

In broad terms, the CRMs and SCMs predicted the same temporal structure for the convective and stratiform rainfall, but some SCMs produced intermittent bursts of higher rainfall, probably because of their relatively large time steps.

It was not possible to make an effective intercomparison of the fluxes of heat and moisture because of major differences in model formulations of surface fluxes; this was identified as being something that needs to be investigated in future years. Momentum fluxes, however, appeared to be similar for most of the models, though one model had appreciably larger values.

The profiles of the divergence of the sensible-heat flux ($Q1$) had similar structures (but not

magnitudes) in all the CRMs and SCMs, with maxima at about 5 km, zero around the tropopause, and negative values in the anvil region. Close to the ground there was a negative region where the rainfall was evaporating. The predicted magnitudes of $Q1$, however, differed substantially between models; two of the CRMs indicated a maximum heating rate of 30 K day^{-1}, whilst the other CRM, and all the SCMs, suggested a maximum of 3–4 times larger than this value.

There was considerable scatter amongst the simulations of the profile of moisture-flux divergence ($Q2$). This was probably related to the complex microphysical processes within the convection, which was represented differently in the different models. Two of the CRMs agreed with one another, but the other CRM gave values that were 5 times higher and were similar to the results of most of the SCMs.

In summary, whilst all the CRMs and SCMs were able to successfully produce simulations of a severe convective storm, it should be noted that Case D was a complex multiscale problem that, for detailed simulation, really required larger computing resources than were available. The storm was exceptionally vigorous and led to appreciable meso/synoptic-scale organization that could not be represented adequately either in the limited horizontal domains used by the CRMs, or in the single-column formats of the SCMs. The SCM parametrizations were probably not able to represent sufficiently well the multiple storm cells within each grid-square column. Also, greater uniformity in the model set-ups was required to enable more detailed intercomparisons to be carried out.

(*e*) *Intercomparison of simulations of Case E by CNRM*

Nine CRMs from groups in the US, Japan and Europe (three of which were funded by EUCREM), and eight SCMs from research groups in Europe were available for intercomparison. Numerous tests were also made to assess the sensitivity of the simulations to ice-phase physics, surface fluxes, radiative processes, domain size and to the use of 2D and 3D models. The large number of models involved in the intercomparison presented a unique opportunity for assessing the ability of CRMs and SCMs to simulate a Pacific squall line.

Cloud-resolving models. All the CRMs were able to simulate the gross features of the squall line, but there were differences related to the different model formulations. Comparison of the time series of maximum upward and downward vertical velocities indicated that the 3D models produced updraughts and downdraughts that were about twice as large as those predicted by the 2D models. However, both types of model indicated that the updraughts were about twice as strong as the downdraughts. There was a marked divergence in time of the evolution of surface rainfall, but the range of values was much the same for most of the 2D and 3D models; in particular, the 3D models that both included ice-phase physics and had open lateral boundary conditions agreed well with one another. The 3D models also gave similar predictions of the stratiform precipitation, except for one model that used periodic lateral boundary conditions; the use of periodic boundary conditions along the axis of propagation of the system within a rather small 100 km domain inhibited the development of stratiform cloud by not allowing the full advection of cloud and rainfall. In contrast, 2D models with periodic lateral boundary conditions within a large 1000 km domain were able to predict stratiform cloud and rain.

The 3D runs were able to produce the evolution of the horizontal structure of the squall line quite well, including its transformation into a hook-shaped feature, and the appearance of horizontal vortices in the northern and southern parts of the system. However the vertical cross sections were different from model to model, but all models with ice-phase physics were able to simulate the double maximum structure as observed by the Doppler radars. The 3D models were also able to reproduce the amplitude and vertical structure of the moist static energy.

The profiles of apparent heat source ($Q1$) due to the convection were similar for all models in both magnitude and vertical structure, as were the predicted profiles of apparent moisture source ($Q2$). However, there were substantial differences between the 2D and 3D models in their simulations of the apparent momentum sources ($Q3^u$, $Q3^v$); the large vertical oscillations in the profiles from the 2D models indicated that the two-dimensional format imposed too strong a constraint on the system.

Single-column models. The SCMs were run with imposed large-scale forcing; this was calculated

from a reference CRM simulation that included ice-phase physics as well as both surface and radiative processes.

The evolution of the surface rainfall in the ensemble of SCM simulations had a spread around the evolution of the rainfall in the reference CRM, but there were large oscillations in the predicted rainfall rates. These tended to disappear when a CAPE closure, rather than a humidity convergence closure, was used for the deep convection scheme, however there was also evidence of inappropriate interactions between the convection scheme and other parametrizations within the models; this was identified as something that needs to be investigated in more detail in the future. Other differences between the SCMs were related to the assumed criteria for triggering the convection. There were also wide differences between the relative amounts of stratiform rainfall predicted by the SCMs (ranging from 0% to 80% of the convective rainfall amounts).

The apparent heat sources ($Q1$), normalized by the total surface rainfall, indicated good agreement with one another, though some SCMs systematically predicted higher or lower values. The agreement between the predictions of the profiles of apparent moisture source ($Q2$) was also fairly good, except at low levels. The vertical structure of $Q3^u$ and $Q3^v$ also agreed broadly with one another (evidently because the squall line had down-gradient momentum transfer that was similar to the way that momentum transport was parametrized in the SCMs) but there were large differences in magnitudes in comparison with the CRM predictions.

8. Benefits and consequences of EUCREM

(a) *Principal benefits*

The EUCREM project has been a highly successful cooperative scientific venture. Observational data from five quite different case-studies have been assembled and distributed on the World-Wide-Web. Simplified profiles, representative of the environmental conditions on each of the occasions, have been defined in forms suitable for use as initial data for running single-column and cloud-resolving models.

Several simulations of each convective case-study have been made using a number of different cloud-resolving models. The results have demonstrated conclusively the ability of such models to represent the main features of the convection present on each of the occasions. Perhaps understandably, the models have been most successful for the stratocumulus and cumulus cases (Cases A and B), though problems remain in correctly simulating the cloud coverage in the cumulus case and drizzle in the stratocumulus case. The question of statistical representivity of the observations and model simulations has also been addressed. The precipitating-convection cases (Cases C, D and E) have presented more difficulties, partly because the mesoscale structures that were intimately linked to the convection were difficult to represent satisfactorily within the somewhat limited model domains used, and partly because of interactions between the intense convection and other parametrized physical processes. Nevertheless, the CRM simulations showed many realistic features. Investigations were made into the sensitivities of the models to resolution, boundary conditions, cloud microphysics, and surface fluxes.

Single-column simulations were made using at least five models for each of the case studies. The evaluation of (and the diagnosis of the weaknesses in) the models has been greatly assisted by the availability of the cloud-resolving model simulations; these have added considerable information about the detailed nature of the convection, over and above what could be ascertained from the basic observational data alone. Overall, the cloud-resolving models have produced reasonable simulations of the EUCREM case-studies, but a substantial number of aspects of the parametrizations have been identified as requiring modification. Some of these have been addressed during the period of the EUCREM contract, but most have been identified as items for future investigation. There is every prospect that on-going research stimulated by the EUCREM project will lead to improvements in convective parametrizations within global models of the atmosphere, resulting in better weather forecasts and climate simulations.

The models employed during EUCREM have varied from those that were already highly developed and well tested (such as the SCMs from CNRM, IMAU and UKMO) to those that were in

an early stage of development (such as the CRM of INM, and the newly coded convective schemes evaluated in the SCMs by LMD and UR). The participating institutes had a range of different interests in the EUCREM project, and included major operational numerical weather prediction centres, leading climate-simulation groups, mesoscale- and cloud-resolving-model specialists, centres with particular interests in observational studies, and smaller groups developing and expanding their skills and expertise. EUCREM has successfully brought together and focused the activities of these groups, and in so doing has encouraged a high degree of interdependency, underpinned by the free exchange ideas and techniques. The success of this inter-institute cooperation, and the enthusiasm for it by the scientists involved, will ensure that the 'EUCREM network' formed during the project will continue for many years in the future.

(*b*) *Model improvements*

Several of the participating groups made modifications and improvements to their modelling systems as a direct consequence of their analyses of the results of numerical simulations produced during the EUCREM project.

(i) *CNRM.*

- Collaboration between CNRM and ECMWF has led to a new way of comparing SCMs and CRMs by using the most reliable CRM to generate large-scale forcing for the SCMs; the SCM simulations are then compared with the reference CRM;
- The need for open (rather than periodic) lateral boundary conditions for simulations of Case E was demonstrated, as was the requirement for a large domain size;
- The use of a closure scheme based on CAPE, rather than on humidity convergence, produced smoother rainfall predictions.

(ii) *DLR.*

- The importance of taking into account significant mesoscale lifting of the atmosphere was demonstrated for Case D; lifting can be responsible for triggering convection in such cases and, as a result, must be taken into account when specifying initial conditions for the simulations;
- The adaption of the MM5 non-hydrostatic mesoscale model for simulating deep convection was successful; several features, such as the horizontal diffusion, were improved during the EUCREM project.

(iii) *ECMWF.*

Shallow convection. Entrainment and detrainment rates for shallow convection were found to be too low, and the predicted cloud fraction was too large.

- A modified scheme has been developed in which the entrainment and detrainment rates are increased to match those in the CRM simulations;
- The SCM now has additional cloud erosion due to the action of turbulent eddies after the air parcel has stopped ascending.

The revised scheme has been tried out on Case B and has produced improvements in the mass flux profile, cloud-base mass flux and cloud fraction (which was an order of magnitude lower). It has also been tried out on a BOMEX case and gave improved results. In a simulation of Case C the cloud fraction remained (correctly) as 100%.

Deep convection. The diagnosed updraught vertical velocity was too large; this gave too long a time for the microphysics to turn cloud water into precipitation, leading to too much statiform, rather than convective, rainfall.

- A modification has been introduced to include, in a simplified way, the effect of the non-hydrostatic vertical pressure gradient; this is done by rescaling the buoyancy term in the calculation to 20% of the total;

- The updraught mass flux has been changed to be defined in terms of parcel buoyancy instead of the large-scale rate of change of moisture;
- Evaporation of precipitation has been changed to occur when the relative humidity is below 100%, instead of 70%.

A rerun gave a smoother increase in rainfall, with convective precipitation being twice as large as stratiform precipitation. The updraught mass profile also agreed well with the CRM simulation.

(iv) *INM.*

- The development of the Meso-NH model has continued, in cooperation with CNRM/GMME;
- The mixing-length formulation has been changed to take into account condensation within the displaced parcels;
- The modified single-column model has been introduced into the Spanish HIRLAM model that is used for weather forecasting; it may become operational after satisfactory testing has been completed.

(v) *KNMI.* The mixed explicit/implicit time-integration scheme in the SCM was very sensitive to the time step used.

- A modified numerical scheme has been developed for the diffusion which uses a fractional time stepping procedure; this allows accurate results to be obtained using relatively large time steps.

(vi) *LMD.*

- The EUCREM case studies have been used to test and evaluate the Emanuel convection scheme. It is judged to have performed well and the scheme is regarded as a good candidate for including in the LMD global climate model.

(vii) *MPIfM.*

- A technique has been developed that enables error bars to be estimated for the observations and the model simulations;
- Ensemble runs of the CRM have demonstrated that the area–time averaging procedure for displaying and validating the CRM simulations can give results having a low statistical reliability; care should be taken to use large eough domains and long enough simulation periods.

(viii) *UKMO.*

- Simulations of the EUCREM cases has assisted in the development of an improved representation of shallow convection.

(ix) *UR.*

- The EUCREM simulations have provided a valuable test of the Betts–Miller convective adjustment scheme in the UGAMP SCM; this may be used in the global climate model after further development.

(*c*) *Proposals for future research*

The EUCREM participants have supported the proposal to hold a workshop in November 1998 to review the project as a whole, to identify the priority areas for future research, and to prepare proposals for new research funding. The following are some of the items that have been mentioned as being important for further investigation.

- dynamical and microphysical interactions in precipitating stratocumulus layers, with particular emphasis on the drizzle processes;
- coupling between convection and other physical processes, such as boundary-layer turbulence—the use of a non-local turbulence scheme;
- mesoscale cellular convection and its relationship to the structure of the boundary layer;
- mechanisms for triggering convection, such as by turbulent eddies, mesoscale circulation systems and forced lifting;
- feedback of the imposed large-scale subsidence onto the structure of the boundary layer;
- entrainment within deep convection;
- entrainment across stratocumulus-topped boundary layers
- entrainment by shallow cumulus—future field experiments to concentrate on this aspect;
- vertical structure of predicted cloud water contents;
- predicted ice-water contents and their relationship to radiative processes;
- representation of convective downdraughts within SCMs;
- parametrization within SCMs of the apparent moisture sources;
- closure assumption for deep convection;
- representation of stratiform cloud associated with mesoscale systems;
- statistical assumptions about the variability of the water content of clouds;
- sensitivity of the predicted cumulus-cloud sizes to the grid length and other model characteristics;
- tracer transports in thunderstorms—NO_x produced by lightning;
- vertical transport of NO_x from the boundary layer by deep convection—impact of aviation on climate.

(*d*) *Scientific papers and reports*

Research during EUCREM is expected to generate a substantial number of scientific papers. The following is a list of some internal reports and papers for publication in the open scientific literature that have been completed or are in the process of being written.

Bechtold, P., Beau, I., Blackburn, M., Brinkop, S., Granpeix, J.-Y., Grant, A., Gregory, D., Guichard, F., Hoff, C. and Redelsperger, J.-L.		An intercomparison of models for a tropical squall line observed during TOGA-COARE. Part 2: Intercomparison of SCMs against CRM results. In preparation
Brown, A. R. and Grant, A. L. M.		A similarity hypothesis for shallow cumulus transports. In preparation
Brown, P. R. A. *et al.*		Precipitating convection in a cold-air outbreak: An intercomparison of cloud-resolving models. In preparation
Chlond, A. and Wolkau, A.		LES of ASTEX RF06: An uncertainty analysis. In preparation
Duynkerke, P. G., Jonker, P. J., Chlond, A., vanZanten, M. C., Cuxart, J., Clarke, P., Sanchez, E., Martin, G., Lenderink, G. and Teixeira, J.		LES and SCM simulations of stratocumulus, and a comparison with observations. In preparation.
Grant, A. L. R. and Brown, A. R.		A parametrization of shallow cumulus for use in a general circulation model. In preparation
Guichard, F., Hoff, C., Redelsperger, J.-L. and Lafore,J. P.	1996	'Cloud-resolving modelling of cloud systems observed during TOGA-COARE'. Pp 266–267 in proceedings of 7th mesoscale conference, Reading, UK
	1997	'Budgets of cloud systems observed during TOGA-COARE'. Pp 168–169 in Proceedings of 22nd AMS Conference on Hurricanes and Tropical Meteorology, Fort Collins,USA
Guichard, F., Lafore, J.-P. and Redelsperger, J.-L.	1996	'Internal behaviour of a deep convective cloud system observed during TOGA-COARE'. Pp 161–162 in Proceedings of 7th Mesoscale Conference, Reading, UK

	1996	'Thermodynamical budgets of an explicitly simulated deep convective cloud system'. Pp 762–765 in Proceedings of 12th International Conference on Clouds and precipitation, Zurich, Switzerland
	1997	Thermodynamical impact and internal structure of a tropical convective cloud system, *Q. J. R. Meteorol. Soc.*, **123**, 2297–2324
Guichard, F., Redelsperger, J.-L. and Lafore, J.-P.	1996	The behaviour of cloud ensemble to external forcings. *Q. J. R . Meteorol. Soc.*, **122**, 1043–1073
Moncrieff M. W., Gregory, D., Krueger, S. K., Redelsperger, J.-L. and Tao, W. K.	1997	GEWEX Cloud System Study (GCSS) Working group 4: Precipitating convective cloud systems. *Bull. Amer. Meteorol. Soc.*, **78**, 831–845
Montmerle Th., Redelsperger, J.-L., Lafore, J.-P., Sommeria, G. and Lemaitre, Y.	1996	'Extended comparisons between airborne Doppler radar data and three-dimensional simulations of a tropical squall line observed during TOGA-COARE'. Pp 790–793 in proceedings of 12th international conference on clouds and precipitation, Zurich, Switzerland
Montmerle Th., Redelsperger, J.-L., Lemaitre, Y. and Lafore, J.-P.	1997	'Three-dimensional simulations of a tropical squall line using two different initializations, including a method based on Doppler radar data: comparisons with observations'. Pp 76–77 in proceedings of 22nd AMS conference on hurricanes and tropical meteorology, Fort Collins, USA
Redelsperger, J.-L	1997	'Cloud-resolving model: Limits and new insights for the parametrization of clouds in GCMs'. Pp 35–42 in Proceedings of Euroclivar workshop on cloud feedbacks and climate change (Eds. C. A. Senior and J. Mitchell)
	1997	'Report on the intercomparison of CRMs and SCMs for the case of squall line observed during TOGA-COARE'. GCSS Science meeting (Dec 97), Boulder, USA. WMO Report to appear
	1997	'Results from the intercomparison of CRMs and SCMs for a TOGA-COARE case (May 97)'. Joint workshop TOGA-COARE and GCSS, Boulder, USA. Report available from the National Center for Atmospheric Research, USA
Redelsperger J.-L., Brown, P., Guichard, F., Hoff, C., Kawashima, Lang, S., Montmerle, Th., Nakumura, Saito, K., Seman, C. and Tao, W. K.	1998	An intercomparison of models for a tropical squall line observed during TOGA-COARE. Part 1: Cloud-resolving models. In preparation
Redelsperger J.-L., Gregory, D., Krueger, S. K., Moncrieff M. W. and Tao, W. K.	1996	'GEWEX Cloud System Study (GCSS) on precipitating convective cloud systems and model intercomparisons. CASE 1: Tropical oceanic convection of TOGA-COARE'. Available from first author or on http://www.cnrm.meteo.fr:8000/gcss/
Redelsperger J.-L. and Guichard, F.	1996	'Detailed analysis of simulated cloud systems observed during TOGA-COARE'. Pp. 58–76 in Proceedings of ECMWF seminar on new insights and approaches to convective parametrization
vanZanten, M. C., Jonker, H. J. J. and Duynkerke, P. G.		Mesoscale fluctuations in scalars generated by boundary layer convection. *J. Atmos. Sci.*, submitted

(e) *Scientific conferences*

The following is a list of some of the presentations about EUCREM that have been made, or are planned to be made, at scientific conferences.

Bechtold P., Beau, I., Blackburn, M., Brinkop, S., Granpeix, J.-Y., Grant, A., Gregory, D., Guichard, F., Hoff, C. and Redelsperger, J.-L.	'GCSS intercomparison of SCMs against CRM results for a squall line observed during COARE'. Clivar/Gewex COARE conference 1998, Boulder, USA
Blackburn, M. and Ioannidou, E.	'The European cloud-resolving modelling programme and development of the Betts–Miller convective parametrization'. 1997 Summer conference of the UK Universities' Global Atmospheric Modelling Programme (UGAMP), University of Reading, UK

Gregory, D. and Guichard, F.	'Revision of ECWMF cloud parametrizations in light of GCSS studies of convection over the IFA of TOGA COARE'. Clivar/Gewex COARE Conference 1998, Boulder, USA
Guichard, F. and Gregory, D.	'On the ability of cloud parametrizations to represent organised convection : a case study contrasting cloud resolving and single column model realizations'. Clivar/Gewex COARE Conference 1998, Boulder, USA
Guichard F., Redelsperger, J.-L., Lafore, J.-P. and Hoff, C.	'Budgets of a few COARE convective systems forced and unforced by convective motions: differences and common features'. Clivar/Gewex COARE Conference 1998, Boulder, USA
Redelsperger J.-L., Brown, P., Donner, L., Guichard, F., Hoff, C., Kawashima, Lang, S., Montmerle, Th., Nakumura, Saito, K., Seman, C. and Tao, W. K.	'GCSS intercomparison of cloud-resolving models for a squall line observed during COARE'. Clivar/Gewex COARE Conference 1998, Boulder, USA

References

Anthes, R. A.	1977	A cumulus parameterization scheme utilizing a one-dimensional cloud model. *Mon. Weather Rev.*, **105**, 270–286
Arakawa, A. and Schubert, W. H.	1974	Interaction of a cumulus cloud ensemble with the large-scale environment. Part I. *J. Atmos. Sci.*, **31**, 674–701
Betts, A. K.	1986	A new convective adjustment scheme. Part I: Observational and theoretical basis. *Q. J. R. Meteorol. Soc.*, **112**, 677–691
Betts, A. K. and Miller, M. J.	1986	A new convective adjustment scheme. Part II: Single column tests using GATE wave, BOMEX, ATEX and arctic air-mass data. *Q. J. R. Meteorol. Soc.*, **112**, 693–709
Browning, K. A.	1996	'The EUCREM project work programme'. Proposal submitted to the European Commission for the European cloud-resolving modelling project
Charney, J. G. and Eliassen, A.	1964	On the growth of the hurricane depression. *J. Atmos. Sci.*,**21**, 68–75
Cuijpers, J. W. P. and Duynkerke, P. G.	1993	Large-eddy simulation of trade-wind cumulus clouds. *J. Atmos. Sci.*, **50**, 3894–3908
Emanuel, K. A.	1994	*Atmospheric convection*. Oxford University Press
Fritsch, J. M. and Chappell, C. F.	1980	Numerical prediction of convectively driven mesoscale pressure systems. Part I: Convective parameterization. *J. Atmos. Sci.*, **37**, 1722–1733
Gregory. D. and Rowntree, P. R.	1989	'A mass flux convection scheme with representation of cloud ensemble characteristics and stability dependent closure'. Dynamical Climatology Tech. Note 81, Available from the Meteorological Office, Bracknell, UK
Krishnamurty, T. N., Ramanathan, Y., Pan, H.-L., Pasch, R. J. and Molinari, J.	1980	Cumulus parameterization and rainfall rates. *Mon. Weather Rev.*, **108**, 465–472
Kuo, H.-L.	1965	On the formation and intensification of tropical cyclones through latent heat released by convection. *J. Atmos. Sci.*, **22**, 40–63
	1974	Further studies of the parameterization of the influence of cumulus convection on the large-scale flow. *J. Atmos. Sci.* **31**, 1232–1240
Manabe, S. Smagorinsky, J. and Strickler, R. F.	1965	Simulated climatology of a general circulation model with a hydrologic cycle. *Mon. Weather Rev.*, **93**, 769–798
Randall, D. A., Xu, K.-M., Somerville, R. J. C. and Iacobellis, S.	1996	Single-column models and cloud ensemble models as links between observations and climate models. *J. Climate*, **9**, 1683–1697
Raymond, D. J. and Blyth, A. M.	1986	A stochastic model for non-precipitating cumulus clouds. *J. Atmos. Sci.*, **43**, 2708–2718
Teidtke, M.	1989	A comprehensive mass flux scheme for cumulus parametrization in large-scale models. *Q. J. R. Meteorol. Soc.*, **117**, 1779–1800

CURRENT JCMM INTERNAL REPORTS

This series of JCMM Internal Reports, initiated in 1993, contains unpublished reports and also versions of articles submitted for publication. The complete set of Internal Reports is available from the National Meteorological Library on loan, if required.

1. **Research Strategy and Programme**
   K A Browning et al
   January 1993

2. **The GEWEX Cloud System Study (GCSS)**
   GEWEX Cloud System Science Team
   January 1993

3. **Evolution of a mesoscale upper tropospheric vorticity maximum and comma cloud from a cloud-free two dimensional potential vorticity anomaly**
   K A Browning
   January 1993

4. **The Global Energy and Water Cycle**
   K A Browning
   July 1993

5. **Structure of a midlatitude cyclone before occlusion**
   K A Browning and N Roberts
   July 1993

6. **Development in Systems and Tools for Weather Forecasting**
   K A Browning and G Szejwach
   July 1993

7. **Diagnostic study of a narrow cold frontal rainband and severe winds associated with a stratospheric intrusion**
   K A Browning and R Reynolds
   August 1993

8. **Survey of perceived priority issues in the parametrizations of cloud-related processes in GCMs**
   K A Browning
   September 1993

9. **The Effect of Rain on Longwave Radiation**
   I Dharssi
   September 1993

10. **Physical Cloud Microprocesses - A Description of the Parametrization used in the Large Eddy Model**
    H Swann
    July 1994

11. **An Appreciation of the Meteorological Research of Ernst Kleinschmidt**
    A J Thorpe
    May 1992

12. **Potential Vorticity of Flow Along the Alps**
    A J Thorpe, H Volkert and Dietrich Heimann
    August 1992

13. **The Representation of Fronts**
    A J Thorpe
    January 1993

14. **A Parametrization Scheme for Symmetric Instability: Test for an Idealised Flow**
C S Chan and A J Thorpe
February 1993

15. **The Fronts 92 Experiment: a Quicklook Atlas**
Edited by T D Hewson
November 1993

16. **Frontal wave stability during moist deformation frontogenesis**
Part 1. Linear wave dynamics
C H Bishop and A J Thorpe
May 1993

17. **Frontal wave stability during moist deformation frontogenesis**
Part 2. The suppression of non-linear wave development
C H Bishop and A J Thorpe
May 1993

18. **Gravity waves in sheared ducts**
C Bishop and A J Thorpe
November 1993

19. **Potential Vorticity and the Electrostatics Analogy: Quasi-Geostrophic Theory**
C Bishop and A J Thorpe
November 1993

20. **Recent Advances in the Measurement of Precipitation by Radar**
A J Illingworth
April 1993

21. **Micro-Physique et Givrage. Cloud Microphysics and Aircraft Icing**
A J Illingworth
May 1993

22. **Differential Phase Measurements of Precipitation**
M Blackman and A J Illingworth
May 1993

23. **Estimation of Effective Radius of Cloud Particles from the Radar Reflectivity**
N I Fox and A J Illingworth
May 1993

24. **A Simple Method of Dopplerising a Pulsed Magnetron Radar**
A Hau, A J Illingworth and J Eastment
November 1993

25. **Radiation and Polar Lows**
George C Craig
February 1994

26. **Collected preprints submitted to the International Symposium on the Life Cycles of Extratropical Cyclones; Bergen, Norway, 27 June - 1 July 1994**
April 1994

27. **Convective Frontogenesis**
Douglas J Parker and Alan J Thorpe
April 1994

28. **Improved Measurement of the Ice Water Content in Cirrus Using a Total Water Evaporator**
Philip R A Brown and Peter N Francis
April 1994

29. **Mesoscale Effects of a Dry Intrusion within a Vigorous Cyclone**
K A Browning and B W Golding
April 1994

30. **GEWEX Cloud System Study, Science Plan**
May 1994

31. **Parametrization of Momentum Transport by Convectively Generated Gravity Waves**
R Kershaw
February 1995

32. **Mesoscale Modelling Newsletter No 5**
May 1994

33. **Observations of the mesoscale sub-structure in the cold air of a developing frontal cyclone**
K A Browning, S A Clough, C S A Davitt, N M Roberts and T D Hewson
May 1994

34. **Longwave Radiative Forcing of a Simulated Tropical Squall Line**
Imtiaz Dharssi
July 1994

35. **On the nature of the convective circulation at a kata-cold front**
K A Browning
September 1994

36. **Collective preprints of papers submitted to the COST-75 International Seminar on Advanced Weather Radar Systems, Brussels, 20-23 September 1994**
November 1994

37. **Use of satellite imagery to diagnose events leading to frontal thunderstorms: Parts 1 and 11 of a case study**
K A Browning and N M Roberts
November 1994

38. **The role of spaceborne millimetre-wave radar in the global monitoring of ice cloud**
P R A Brown, A J Illingworth, A J Heymsfield, G M McFarquahar, K A Browning and M Gosset
December 1994

39. **Potential Vorticity Inversion**
Michael Ziemianski
October 1994

40. **Theory of mature tropical cyclones; a comparison between Kleinschmidt (1951) and Emanuel (1986)**
Suzanne L Gray
December 1994

41. **Dispersion and removal of pollutants during the passage of an atmospheric frontal system**
N R Gimson
December 1994

42. **The role of snow sublimation in frontogenesis**
D J Parker and A J Thorpe
December 1994

43. **Potential vorticity and the electrostatics Analogy: Ertel-Rossby formulation**
A J Thorpe and C H Bishop
December 1994

44. **Mesoscale aspect of extratropical cyclones: an observational perspective**
K A Browning
January 1995

45. **A Polar Low Outbreak: Evolution and Mesoscale Structures**
T D Hewson, G C Craig and C Claud
February 1995

46. **Generation of near-surface gusts of deep convection**
K Nakamura and R Kershaw
April 1995

47. **Attribution Concepts applied to the Omega Equation**
S A Clough, C S A Davitt and A J Thorpe
June 1995

48. **Parametrization of mixed-phase cloud and precipitation**
Susan P Ballard and M Gerard Hutchinson
June 1995

49. **Short-range forecasting of stratocumulus: Initialization Prediction**
Susan Ballard, Simon D Jackson and B Macpherson
June 1995

50. **Contributions of the JCMM/Dept of Meteorology Radar Group to the 27th AMS Radar Meteorology Conference, Vail October 1995**
June 1995

51. **Cold Pools in Shear**
Douglas J Parker
September 1995

52. **High-resolution analysis of frontal fracture**
K A Browning, S P Ballard and C S A Davitt
September 1995

53. **The Albedo of Broken Cloud Fields: Calculations using a modified two stream radiation code**
Imtiaz Dharssi and Roy Kershaw
October 1995

54. **Parametrization of momentum transport by convection. I: Theory and cloud modelling results**
R Kershaw and D Gregory
November 1995

55. **Variation of frontal structure along a cold front**
K A Browning and N M Roberts
November 1995

56. **Secondary Frontal Waves**
Douglas Parker
December 1995

57. **Objective Fronts**
T D Hewson
March 1996

58. **Mesoscale analysis of the activation of a cold front during cyclogenesis**
K A Browning, N M Roberts and A J Illingworth
June 1996

59. **Investigation of Different Representations of Rain in a 1-d Evaporation Model**
H Swann
May 1996

60. **Parametrization of diabatic processes in the inversion of the omega-equation**
M Athanassiadou and A J Thorpe
June 1996

61. **The Role of the Environmental Flow in the Development of Secondary Frontal Cyclones**
I A Renfrew, A J Thorpe and A Joly
June 1996

62. **Consequences of the geostrophic momentum approximation on barotropic instability**
S Malardel, A J Thorpe and A Joly
June 1996

63. **Contributions to the AMS/RMS Conference on Mesoscale Processes**
Reading, 9-13 September 1996

64. **Vorticity and Potential Vorticity in Stratified Flows Interacting with an Isolated Obstacle**
Jorge A Gutiérrez and A J Thorpe
September 1996

65. **Triple Point Development: Two Case Studies**
Douglas Parker
September 1996

66. **Radar observations of wind-shear splitting within evolving atmospheric Kelvin-Helmholtz billows**
D Chapman and K A Browning
April 1997

67. **Cold Frontal Structure derived from radar wind profilers**
K A Browning, D Jerrett, J Nash, T Oakley, N M Roberts
May 1997

68. **The dry intrusion and its effect on the frontal, cloud and precipitation structure of extratropical cyclones**
K A Browning - Text of invited special lecture at the Spring Conference
of the Meteorological Society of Japan, University of Tsukuba, 22 May 1997

69. **Met. Office Unified Model data, diagnostic graphics programs, and other observational data available from the JCMM through the aegis of the Universities Weather Research Network (UWERN).** (Plus supplement)
Peter Panagi and Ed Dicks
June 1997

70. **Contributions of the JCMM/Dept of Meteorology Radar Group to 28th AMS Radar Meteorology Conference.** Austin, Texas
September 1997

71. **Sensitivity of short-range weather forecasts to local potential vorticity modifications**
Meral Demirtas and Alan Thorpe
July 1997

72. **Objective identification of frontal wave cyclones**
T D Hewson
August 1997

73. **Attribution and its application to mesoscale structure associated with tropopause folds**
A J Thorpe
September 1997

74. **The Role of the Environmental Flow in the Development of Secondary Frontal Cyclones**
Ian A Renfrew, Alan J Thorpe and Craig H Bishop
September 1997

75. **Potential Vorticity: A short history of its definitions and uses**
Alan J Thorpe and Hans Volkert
September 1997

76. **Superposing Semi-Geostrophic Potential Vorticity Anomalies**
H R Birkett and A J Thorpe
September 1997

77. **Short period forecasting of catchment-scale precipitation.**
Part 1: the role of Numerical Weather Prediction
M A Pedder, M Haile and A J Thorpe
September 1997

78. **Verification of the Tracking Technique Used in an Experimental Cloud Motion Wind Inferring System**
Z Wang, K A Browning and G A Kelly
October 1997

79. **A Preliminary Study of Fourier Series Analysis for Cloud Tracking with GOES High Temporal Resolution Images**
Z Wang
October 1997

80. **Analysis of an ex-tropical cyclone after reintensifying as a warm-core extratropical cyclone**
K A Browning, G Vaughan and P Panagi
November 1997

81. **A JCMM overview of FASTEX IOPs**
S A Clough, H W Lean, N M Roberts, H Birkett, J-P Chaboureau, R Dixon, M Griffiths, T D Hewson and A Montani
January 1998

82. **Programs for PV Inversion and Modification**
Meral Demirtas
December 1997

83. **Release of potential shearing instability in warm frontal zones**
D Chapman and K A Browning
February 1998

84. **The European Cloud-Resolving Modelling Programme (EUCREM)**
Summary Report from the coordinator
P W White
April 1998

Met Office Joint Centre for Mesoscale Meteorology Department of Meteorology
University of Reading PO Box 243 Reading RG6 6BB United Kingdom
Tel: +44 (0)118 931 8425 Fax: +44 (0)118 931 8791
www.metoffice.com